

JGR Solid Earth

RESEARCH ARTICLE

10.1029/2021JB023329

New Magnetic Anomaly Constraints on the Antarctic Crust

H. R. Kim¹ , A. V. Golynsky² , D. A. Golynsky² , H. Yu¹ , R. R. B. von Frese³, and J. K. Hong⁴ 

Key Points:

- Swarm satellite magnetic gradient anomaly observations provide useful constraints to help fill regional coverage gaps in the more than 3.5 million line-km of ship and airborne magnetic anomaly data of the ADMAP-2 compilation. They also substantially enhance Antarctic crustal studies of the near-surface magnetic survey data
- Onshore, the ADMAP-2 anomalies over West Antarctica include the effects of extensive late Cenozoic volcanic rocks within the West Antarctic Rift System and Mesozoic arc magmatism and terrane accretion along the paleo-Pacific active margin of Gondwana. Over East Antarctica, they mark the Mawson Craton's southernmost boundary along 85.5°S between 157°E to 135°E to suggest that the Shackleton Ranges may not be part of the craton (Boger, 2011)
- Offshore, the ADMAP-2s anomalies illuminate Antarctica's continent-ocean transition zones. Satellite magnetic anomaly maxima also map enhanced crustal heat flow variations that yield relatively marginal signatures in the near-surface observations

Correspondence to:

H. R. Kim,
kimhr@kongju.ac.kr

Citation:

Kim, H. R., Golynsky, A. V., Golynsky, D. A., Yu, H., von Frese, R. R. B., & Hong, J. K. (2022). New magnetic anomaly constraints on the Antarctic crust. *Journal of Geophysical Research: Solid Earth*, 127, e2021JB023329. <https://doi.org/10.1029/2021JB023329>

Received 6 SEP 2021
Accepted 19 FEB 2022

© 2022. The Authors.

This is an open access article under the terms of the [Creative Commons Attribution-NonCommercial-NoDerivs License](https://creativecommons.org/licenses/by-nc-nd/4.0/), which permits use and distribution in any medium, provided the original work is properly cited, the use is non-commercial and no modifications or adaptations are made.

¹Department of Geoenvironmental Science, Kongju National University, Gongju, Republic of Korea, ²VNIIOkeangeologia, All-Russian Scientific Research Institute for Geology and Mineral Resources of the World Ocean, St. Petersburg, Russia, ³School of Earth Sciences, The Ohio State University, Columbus, OH, USA, ⁴Korea Polar Research Institute, Incheon, Republic of Korea

Abstract The Antarctic Digital Magnetic Anomaly Project's first-generation magnetic anomaly map (ADMAP-1) was produced for the region south of 60°S from about 1.5 million line-kms of airborne and marine magnetic anomaly data (Golynsky et al., 2001; <https://www.bas.ac.uk/data/our-data/maps/thematic-maps/admap-magnetic-anomaly-map-of-the-antarctic/>). The second-generation ADMAP-2 compilation (Golynsky et al., 2017; <https://doi.org/10.22663/ADMAP.V2>) incorporated an additional roughly 2.0 million line-kms of airborne and marine magnetic anomaly data from international mapping through 2015. The present study integrates satellite magnetic observations from the Swarm mission with the near-surface data of ADMAP-2 to help fill the regional coverage gaps and better define the altitude behavior of the Antarctic's magnetic anomalies for enhanced geological analysis. The resulting satellite magnetic data-supplemented compilation, ADMAP-2s, yields further constraints on the enigmatic geology of the Gamburtsev Subglacial Mountains, Prince Charles Mountains, Wilkes Land, Dronning Maud Land, and other poorly explored Antarctic areas. It offers insights on the global tectonic processes and crustal properties of the Antarctic and helps to unify disparate geologic and geophysical studies by linking widely separated outcrops. It also supports studies on the geological controls of the Antarctic ice sheet, the crustal transitions between Antarctica and the adjacent oceans, and the geodynamic evolution of the Gondwana and Rodinia supercontinents.

Plain Language Summary This study integrates the second-generation magnetic anomaly compilation with Swarm satellite magnetic data to offer important new constraints on the geology of the Antarctic's crust that is largely hidden beneath a pervasive blanket of seawater, ice, and snow. The satellite data-supplemented magnetic anomaly compilation links widely separated outcrops to facilitate enhanced understanding of the lithospheric transition between Antarctica and its adjacent oceans, as well as the Antarctic's role in the tectonic evolution of the Gondwana and Rodinia supercontinents. The satellite data-supplemented magnetic anomaly compilation in combination with complementary geological information, and ice-probing radar, gravity, and other geophysical data enhances understanding Antarctic crustal rifting, mountain building and basin formation, plate subduction and accretion, and other regional lithospheric processes.

1. Introduction

Magnetic surveying provides a very effective window on the snow-, ice-, and seawater-covered crustal geology of the Antarctic south of 60°S as generalized in Figures 1 and 2. Thus, to support these crustal studies, national geomagnetic survey campaigns were initiated with the 1957–1958 International Geophysical Year (IGY). However, they lacked international coordination so that tracking the survey coverages and progress was limited. This also made it difficult to appreciate the regional geologic settings of the surveys and plan for new ones. Accordingly, to better coordinate international geomagnetic surveying of the Antarctic and conserve the data for geological studies, the Antarctic Digital Magnetic Anomaly Project (ADMAP) was initiated in 1995 following resolutions from the Scientific Committee on Antarctic Research (SCAR) and the International Association of Geomagnetism and Aeronomy (IAGA; Chiappini & von Frese, 1999; Chiappini et al., 1998; Johnson et al., 1997).

ADMAP released its first magnetic anomaly compilation, ADMAP-1, and near-surface anomaly grid (Figure 3) some 6 years after its launch (Golynsky et al., 2001). The compilation included more than 1.5 million line-km of ship and airborne magnetic measurements that were collected from the IGY'1957–1958 through 1999 along with some 5.6 million line-km of Magsat satellite crustal magnetic observations. Magsat data from the roughly

Author Contributions:

Conceptualization: H. R. Kim, A. V. Golynsky
Data curation: H. R. Kim, A. V. Golynsky, D. A. Golynsky
Formal analysis: H. Yu, R. R. B. von Frese, J. K. Hong
Funding acquisition: H. R. Kim, J. K. Hong
Investigation: H. R. Kim, A. V. Golynsky, D. A. Golynsky, H. Yu, R. R. B. von Frese
Methodology: H. R. Kim, D. A. Golynsky, H. Yu, R. R. B. von Frese
Project Administration: A. V. Golynsky, R. R. B. von Frese
Software: H. R. Kim
Supervision: R. R. B. von Frese, J. K. Hong
Validation: J. K. Hong
Visualization: H. R. Kim, A. V. Golynsky
Writing – original draft: H. R. Kim, A. V. Golynsky, D. A. Golynsky, R. R. B. von Frese
Writing – review & editing: A. V. Golynsky, R. R. B. von Frese

half-year satellite mission provided unique regional crustal anomaly perspectives. They also facilitated predicting anomaly values within the large coverage gaps in the near-surface surveys by joint inversions of the satellite and surrounding near-surface magnetic observations (Kim et al., 2004). Follow-on efforts improved the gap estimates using the more accurate and comprehensive post-Magsat magnetic observations from the multi-year Ørsted and Champ satellite missions (Kim et al., 2007; von Frese et al., 2008).

In 2008, NOAA's National Centers for Environmental Information (<https://www.ngdc.noaa.gov>) archived the ADMAP-1 grids and supplemental near-surface survey data for public distribution. The Korea Polar Research Institute (<http://admap.kopri.re.kr>) also provides free public access to the Magsat-, Ørsted-, and Champ-augmented grids along with the near-surface survey data.

ADMAP-1 also contributed Antarctic coverage for the World Digital Magnetic Anomaly Map (WDMAM; Maus et al., 2009). However, WDMAM incorporated only the shorter wavelength components of ADMAP-1 under the dubious proposition that the compilation's long-wavelength anomalies must conform with the near-surface predictions of the satellite magnetic observations. Specifically, WDMAM replaced the surveyed anomalies with wavelengths greater than about 400 km in the ADMAP-1 grid by the nonunique and poorly constrained anomaly estimates downward continued over several hundred kms from the orbital measurements.

However, von Frese et al. (2013) found that this substitution corrupted ADMAP-1's contributions to WDMAM's south polar predictions mainly because measurement and data processing errors substantially limit the near-surface sensitivity of satellite anomaly observations. In general, by the equivalent source and non-uniqueness attributes of potential fields, the reliability of any magnetic model's anomaly prediction decreases with increasing distance from the constraining observations (e.g., Hinze et al., 2013). Thus, the veracity of near-surface anomaly predictions from satellite-only magnetic measurements is extremely limited (e.g., Kim & von Frese, 2017; von Frese et al., 2013).

Furthermore, the state-of-the-art data processing for both the first- and second-generation ADMAP near-surface anomaly grids revealed no significant long-wavelength errors. The data processing included extensive statistical and visual screening of the data inputs and outputs for errors at all spatial and temporal scales (Golynsky et al., 2001, 2017; Golynsky, Golynsky, & von Frese, 2021 in-review). Data were discarded only in the limited number of cases where they were irreconcilable. Thus, the data processing in both compilations incorporated nearly all of the available near-surface survey data for effective grid estimates of the long-wavelength anomaly components. Confidence in the gridded regional anomaly components is further bolstered by the general lack of reports to date from the public on significant data errors in either of the two published compilations.

In geological application, ADMAP-1 provided significant new constraints on the crustal attributes of south polar Proterozoic-Archean cratons, Proterozoic-Paleozoic orogens, and Phanerozoic magmatic arcs and rifts. It helped to map large igneous provinces like the Ferrar dolerites that extend hundreds of kilometers beyond their famous cliff exposures along the Transantarctic Mountains (TAM), and confined the Kirkpatrick basalts mostly to the Polar Plateau's edge in the central TAM and parts of Victoria Land (e.g., Ferraccioli et al., 2000, 2002, 2003, 2009; Finn et al., 1999; Studinger et al., 2003).

The release of the second-generation ADMAP-2 compilation in Figure 4 (Golynsky et al., 2017) revealed substantially expanded near-surface geomagnetic survey coverage, particularly in East Antarctica and its offshore areas. The production of this compilation involved processing more than 2 million line-km of new marine and airborne magnetic survey data that were then merged with ADMAP-1's roughly 1.5 million line-km of data. The datasets in the second-generation compilation provided further important details on the Antarctic's basement terranes and the intervening suture zones, intra-continental and continental margin rift basins, and regional plutonic and volcanic features like the Ferrar dolerites and Kirkpatrick basalts (e.g., Aitken et al., 2016; Ferraccioli & Bozzo, 2003; Ferraccioli et al., 2011; Golynsky, Golynsky, et al., 2006; Goodge & Finn, 2010; Mieth et al., 2014).

To enhance geological applications, the present study supplements the ADMAP-2 compilation with the magnetic gradient observations from the multi-year Swarm mission's constellation of three low-earth orbiting satellites (Haagmans et al., 2010). Accordingly, the next section develops the ADMAP-2s compilation where supplemental satellite magnetic data help fill the regional gaps in the near-surface survey coverage and establish boundary conditions to better image the spatial attributes of the anomalies from near-surface through satellite altitudes.

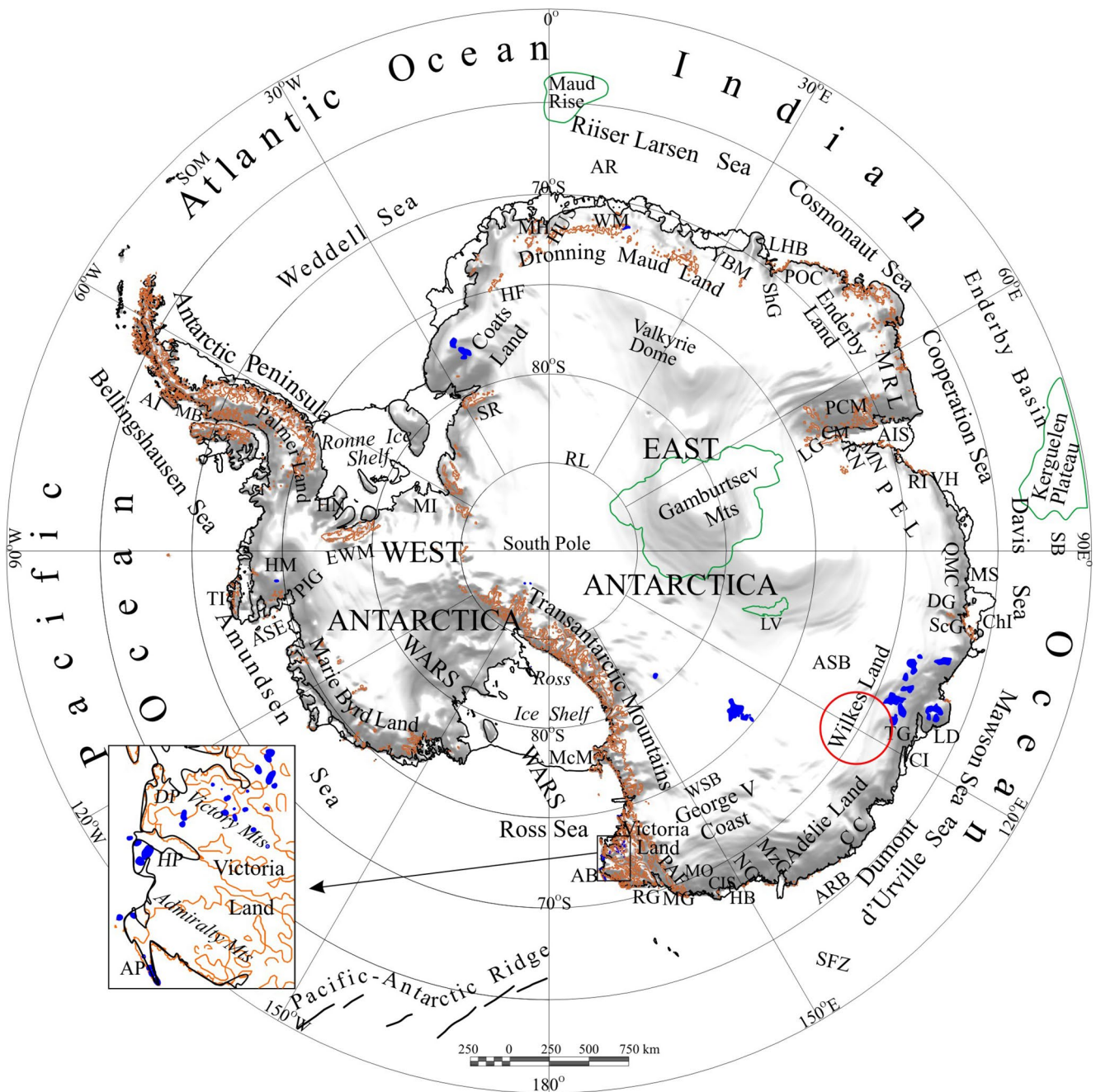


Figure 1. Shaded relief map of Antarctica's surface topography showing selected geographical and geological features described in this study. Blue patches highlight the distribution of the intensely negative near-surface magnetic anomalies that the text attributes to reversed natural remanent magnetizations of intrusive and volcanic rocks. The insert emphasizes their distribution over Victoria Land. Brown contours delineate outcrops, and green contours outline the subglacial Lake Vostok (LV) and Gamburtsev Mountains, as well as the Maud Rise and Kerguelen Plateau. The red circle locates the putative Wilkes Land impact basin, and Table 1 lists the geological and geographic name abbreviations.

2. ADMAP-2s Data Processing

The coverage gaps between the near-surface surveys in Figure 4 are particularly extensive in East Antarctica and the Pacific area north of West Antarctica and the Ross Sea. However, potential field anomaly continuation is a boundary value problem so that weighted local measurements of both near-surface and satellite-altitude observations are effective for estimating gap-filling magnetic anomaly values (Kim et al., 2007). Accordingly, each

Table 1
Antarctic Geologic and Geographic Abbreviations in Figures 1 and 2

AI	Adelaide island	MN	Manning Nunataks
AIS	Amery Ice Shelf	MO	Mount Obruchev
AP	Adare Peninsula	MRL	MacRobertson Land
AR	Astrid Ridge	MS	Mirny Station
ARB	Adélie Rift Block	MzG	Mertz Glacier
ASB	Aurora Subglacial Basin	NG	Ninnis Glacier
ASE	Amundsen Sea Embayment	PCM	Prince Charles Mountains
CC	Clarie Coast	PEL	Princess Elizabeth Land
ChI	Chugunov Island	PIG	Pine Island Glacier
CI	Chick Island	POC	Prince Olav Coast
CIS	Cook Ice Shelf	QMC	Queen Mary Coast
CM	Clemence Massif	RG	Rennick Graben
DG	Denman Glacier	RI	Rauer Islands
DP	Daniel Peninsula	RL	Recovery Lakes
EWM	Ellsworth-Whitmore Mountains	RN	Robertson Nunatak
HB	Horn Bluff	ScG	Scott Glacier
HF	Heimefrontfjella	SFZ	Spenser Fracture Zone
HM	Hudson Mountains	ShG	Shirace Glacier
HN	Haag Nunatak	SOM	South Orkney Microcontinent
HP	Hallett Peninsula	SR	Shackleton Range
HUS	H.U. Sverdrupfjella	TG	Totten Glacier
LD	Low Dome	TI	Thurston Island
LG	Lambert Glacier	VH	Vestfold Hills
LHB	Lützow-Holm Bay	WARS	West Antarctic Rift System
LV	Lake Vostok	WM	Wohltat Massif
McM	McMurdo	WSB	Wilkes Subglacial Basin
MG	Matusевич glacier	YBM	Yamato-Belgica Mountains

gap was filled in with the predictions from a local point dipole model constrained jointly by the satellite crustal magnetic anomaly estimates in Figure 5 from the Swarm mission (Olsen et al., 2017) and the near-surface anomaly observations around the gap's perimeter (Kim et al., 2004, 2007; Yu et al., 2019).

To facilitate spherical coordinate modeling efforts, the gap-filled ADMAP-2 grid of magnetic anomalies at the variable altitudes of the composite surveys (Golynsky et al., 2017) was differentially continued to the Earth's mean geocentric radius of 6,371.2 km using the CompuDrape extension from Geosoft's Oasis montaj geopotential anomaly processing software (Paterson et al., 1990). Figure 6 gives the resulting differentially continued, gap-filled ADMAP-2 grid, where the gap-filling predictions require careful use because they are not unique and propagate data measurement and processing errors.

The gap-filled ADMAP-2 grid was then modeled by an array of equivalent point sources (EPS) with spherical coordinate magnetic effects (Asgharzadeh et al., 2008; Hinze et al., 2013; von Frese, 1998; von Frese et al., 1981) that also satisfied the Swarm magnetic anomalies as an orbital-altitude boundary condition. Here, the EPS inversion of the near-surface and satellite data obtained least squares magnetic susceptibility estimates for the (97,052 × 93,456)-array of point magnetic dipoles distributed over the study area in roughly 20-km intervals at the uniform depth of 30 km below the Earth's mean geocentric radius of 6,371.2 km. The resultant ADMAP-2s model honors the near-surface anomalies with the root-mean-squared difference of RMSD = 18.50 nT and correlation coefficient of CC = 0.970, and the satellite anomalies with the RMSD = 1.58 nT and CC = 0.967.

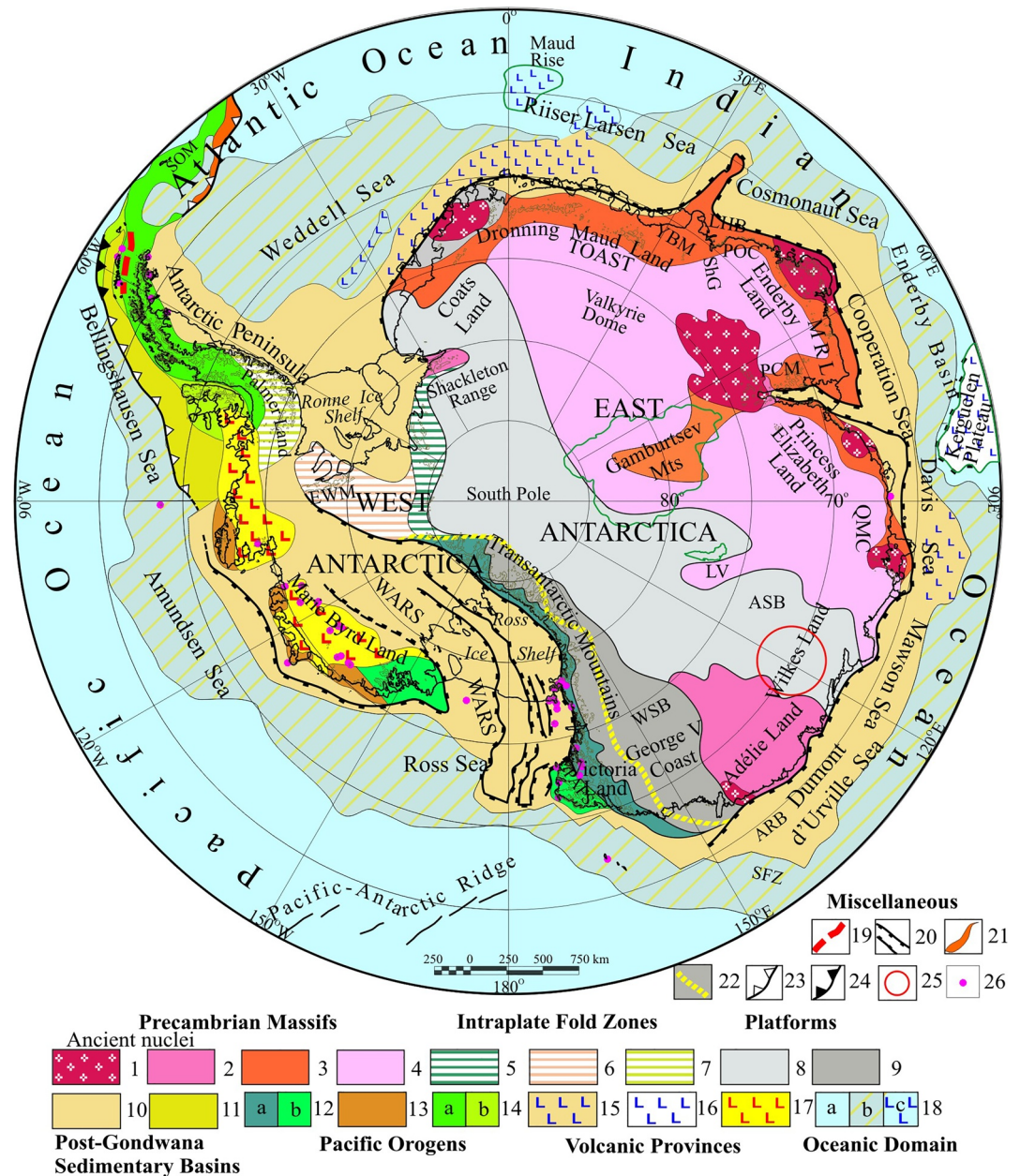


Figure 2. Crustal geology of the Antarctic south of 60°S inferred from outcrop, drilling, and geophysical observations as modified from Grikurov and Leychenkov (2012) and Zhang et al. (2020). Table 1 alphabetically lists the feature abbreviations and Table 2 describes the legend.

Thus, the ADMAP-2s compilation provides improved perspectives on how the crustal magnetic anomalies may vary over the intervening altitudes that simply are not available from standard downward or upward continuations of the individual datasets. Consider, for example, estimating at Swarm's approximate resolution limit of about 250 km the regional anomalies in the gap-filled near-surface anomaly grid of Figure 7a from the downward continued Swarm magnetic anomalies in Figure 7b. Here, both maps were low-pass filtered for 250+ km wavelengths to facilitate the comparison. However, the correlation coefficient between them of $CC(A,B) = 0.64$ indicates that the Swarm mission captured slightly less than 41% of the regional near-surface surveyed anomalies with the differences given in Figure 7c.

Table 2
Legend for Figure 2

Feature	#	Description		Feature	#	Description			
Precambrian Massifs	1	Archean		Table 2: Legend for Figure 2.					
	2	Paleoproterozoic							
	3	Mesoproterozoic							
	4	Undifferentiated							
Intraplate Fold Zones	5	Early Paleozoic					Volcanic Provinces	15	Jurassic-Cretaceous (volcanic margins)
	6	Late Paleozoic - Early Mesozoic						16	Cretaceous (Kerguelen microcontinent)
	7	Late Mesozoic						17	Late Cenozoic (plateau basalts of West Antarctic Rift Zone)
Platforms	8	Neo(?) Proterozoic - Early Mesozoic					Oceanic Domain	18	a - Sediment starved
	9	Middle Paleozoic - Early Mesozoic (Gondwana System)							b - affected by increased terrigenous supply (thickness of Late Mesozoic - Cenozoic sediments in excess of 1 km)
Post-Gondwana Sedimentary Basins	10	Mesozoic - Cenozoic (breakup-related)							c - Late Jurassic-Cretaceous plateaus
	11	Cenozoic (forearc)		19	Incipient seafloor spreading				
Pacific Orogens	12	Early Paleozoic	a - Ross Orogen	Miscellaneous	20	Rift boundaries			
			b - Borchrevink Orogen		21	Neogene island arc			
	13	Paleozoic - (?)Early Mesozoic (Amundsen Orogen)			22	Ross orogen's inboard boundary			
	14	Late Paleozoic - Cenozoic (Andean Orogen)	a - Early Mesozoic		23	Paleosubduction zone			
			b - Late Mesozoic-Cenozoic		24	Active subduction zone			
25	Wilkes Land impact basin								
26	Vocano								

Comparable unreliability issues accompany the upward continuations of the near-surface anomalies to satellite altitudes such as shown in Figure 7d, where the EPS continuation of the near-surface magnetic data in Figure 6 attempts to predict the Swarm anomalies of Figure 7e. Here, the $CC(C, D) = 0.45$ suggests that the upward continued anomaly estimates capture only about 20% of Swarm's anomalies at the mission's average orbital altitude of 250 km above the Earth's mean geocentric radius with the differences given in Figure 7f. Clearly, substantial reliability limitations challenge uses of near-surface potential field variations inferred from satellite observations and vice versa.

However, as a boundary value problem, potential field anomaly continuation can be carried out with models that satisfy multi-altitude anomaly datasets (e.g., Hinze et al., 2013; Kim & von Frese, 2017; Kim et al., 2013; von Frese et al., 2013). For example, Figure 8 reveals perspectives on the Antarctic's total intensity magnetic field anomalies over geocentric altitudes ranging from 25 through 200 km via the EPS-model that largely accounts for both the near-surface and Swarm anomalies in Figures 7a and 7d, respectively.

These results provide insights into the altitude behavior of the crustal anomalies that simply are inaccessible to conventional single-surface upward continuations of the ADMAP-2 grid and downward continuations of the Swarm data. However, they lack uniqueness and can vary as new measurements are obtained. For example, actual surveying at 75 km altitude may map a flat and unvarying field of zero or some other constant amplitude in stark contrast to Figure 8c's predictions. The newly mapped data accordingly define a third boundary condition that may be integrated with the near-surface and Swarm boundary values by joint inversion for an EPS model, which now essentially satisfies the three boundary conditions with appropriately updated anomaly estimates at the intervening altitudes. Clearly, the magnetic anomaly results from this study must be used with care because they are not unique and also propagate data measurement and processing errors. The next section considers some of their implications concerning the Antarctic's crustal geology.

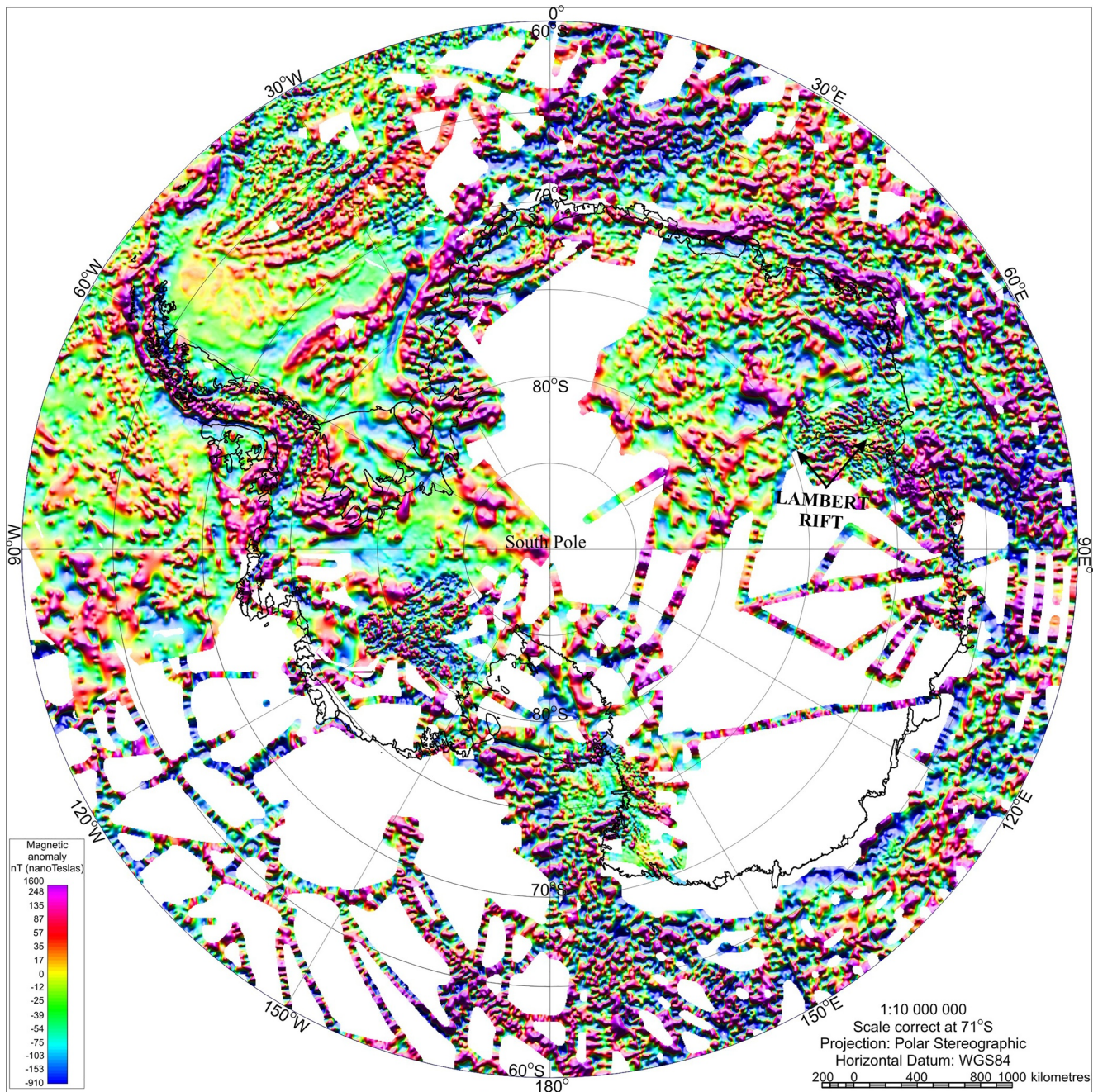


Figure 3. The Antarctic Digital Magnetic Anomaly Project's first-generation map (ADMAP-1) of near-surface scalar total field magnetic anomalies in polar stereographic projection with central meridian = 0°E longitude and standard parallel = -71°S latitude (Golynsky et al., 2001). Generated from roughly 1.5 million line-km of airborne and shipborne magnetic observations, the 5-km grid of data at the variable altitudes of the composite surveys was low-pass filtered for about 10+ km wavelengths.

3. Discussion

This section reviews the ADMAP-2s near-surface anomaly map (Figure 6) and its satellite-constrained predictions with increasing altitudes (Figure 8) for further insights on the plate tectonic processes and crustal properties of the Antarctic south of 60°S. The magnetic anomaly compilation links widely separated outcrops to help draw together disparate geologic studies of the continental interior (Ferraccioli et al., 2009; Gohl et al., 2013; Golynsky, 2007; Goodge & Finn, 2010; Jordan et al., 2014; Mieth & Jokat, 2014). Offshore, it illuminates Antarctica's continent-ocean transition zones. In general, ADMAP-2s provides the most comprehensive and powerful data set

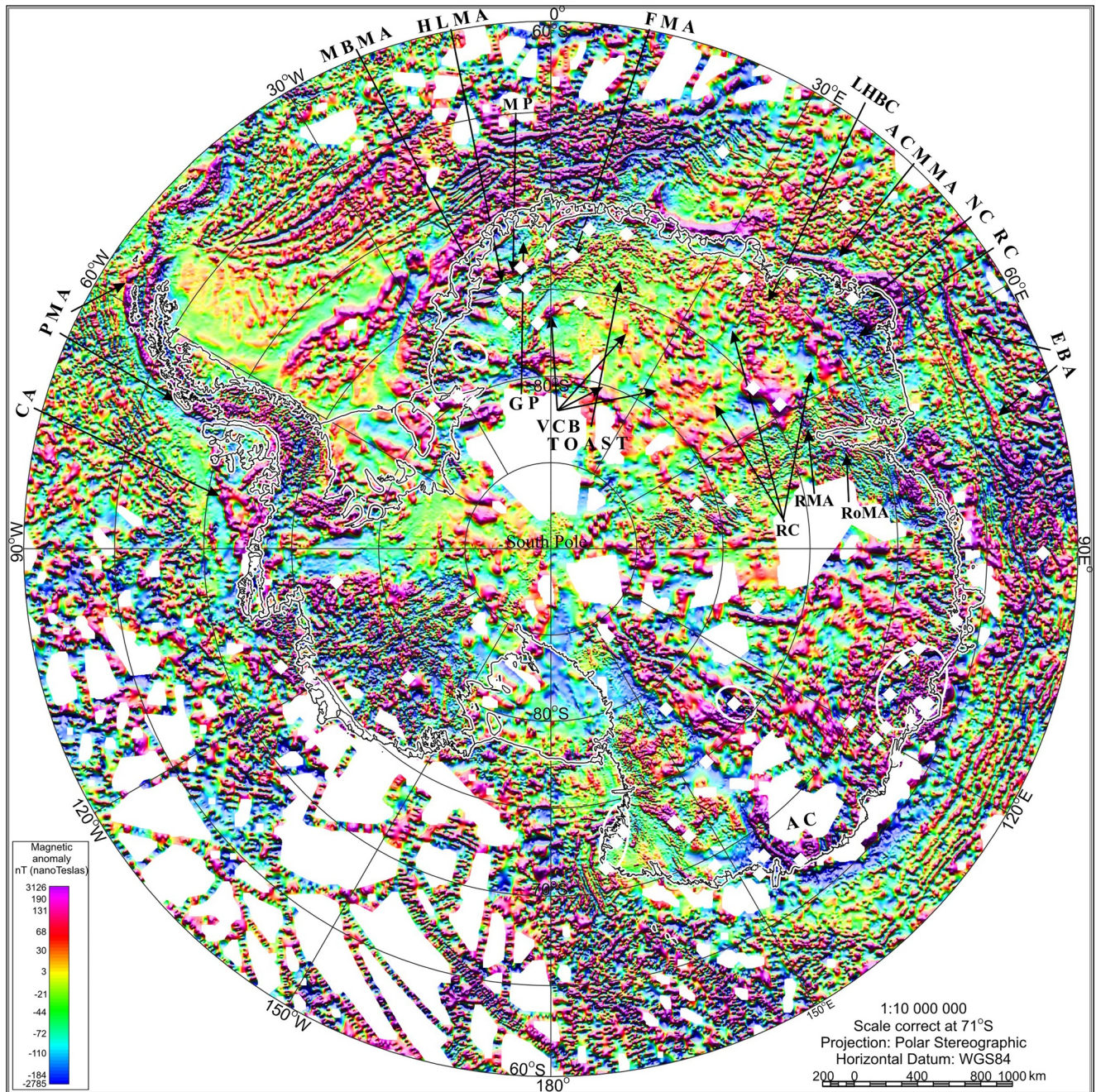


Figure 4. The Antarctic Digital Magnetic Anomaly Project's second-generation map (ADMAP-2) of near-surface scalar total field magnetic anomalies in shaded relief on a polar stereographic projection with central meridian = 0°E longitude and standard parallel = -71°S latitude (Golynsky et al., 2017). Generated from roughly 3.5 million line-km of airborne and shipborne magnetic observations, the 1.5-km grid of anomalies at the variable altitudes of the composite surveys was low-pass filtered for about 10+ km wavelengths. The four white ellipses in East Antarctica encompass the intensely negative magnetic anomalies discussed in the text. Anomaly and geographic name abbreviations include: **ACMMA** – Antarctic Continental Margin Magnetic Anomaly; **EBA** – Enderby Basin Anomaly; **FMA** – Forster Magnetic Anomaly; **GP** – Grunehogna Province; **HLMA** - Heimefront Lineament Magnetic Anomaly; **MBMA** – Maud Belt of Magnetic Anomalies; **NC** – Napier Complex; **PMA** – Pacific Margin Anomaly; **RC** – Ruker Complex; **RMA** – Ruker Magnetic Anomaly; **RoMA** – Robertson Magnetic Anomaly; **TOAST** – Tonian Oceanic Arc Superterrane; **VCB** – Valkyrie Cratonic Block. The bold white-filled diamond symbols mark the ‘centered roughly at’ (cra) coordinates for the applicable magnetic anomalies numerically annotated in the text and Figure 5.

yet developed that together with the crustal geochronology and other geological constraints may help to refine Antarctica's tectonic evolution during the assembly and break-up of the Gondwana and Rodinia supercontinents (Aitken et al., 2014, 2016; Davey et al., 2016; Gohl et al., 2013; Granot et al., 2013; Jordan et al., 2017; König

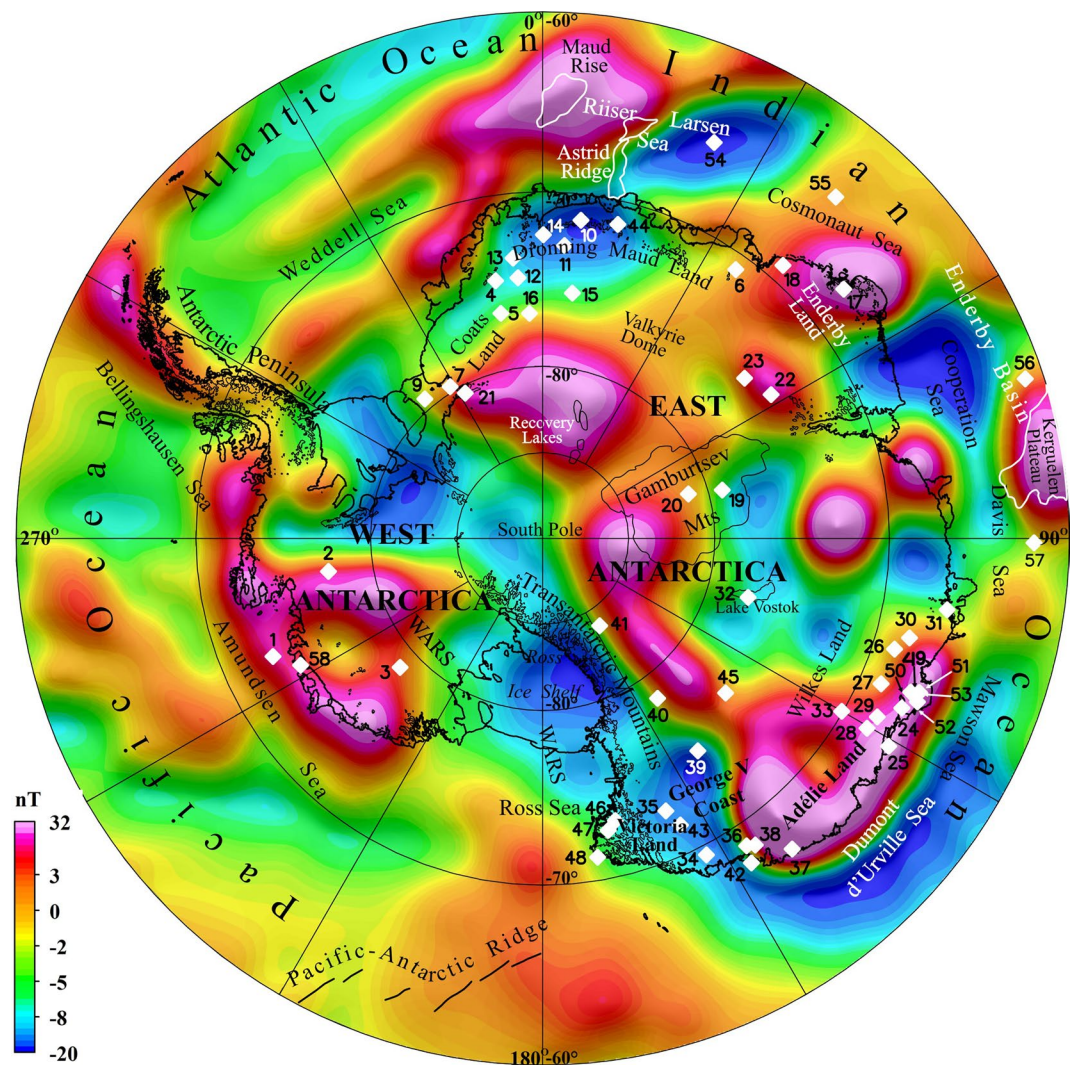


Figure 5. Swarm total magnetic field anomaly estimates (Olsen et al., 2017) at the grid interval of 0.5° for the Antarctic crust south of 60°S at 250 km above the Earth's mean geocentric radius of 6,371.2 km. Superposed are relevant geological/geographic features from Figure 1, and numbered bold white-filled diamond symbols that mark the 58 cra coordinates from Figure 4 as numerically annotated in the text.

& Jokat, 2006; Leinweber & Jokat, 2012). The subsections below expand on the geological interpretations of the compilations from ADMAP-1 (Chiappini & von Frese, 1999; Ferraccioli et al., 2013; von Frese et al., 2002) and ADMAP-2 (Golynsky et al., 2017) to emphasize the geological utility of the ADMAP-2s compilation for West and East Antarctica and the Southern Ocean.

3.1. West Antarctic Magnetic Anomalies

The ADMAP-2s near-surface grid (Figure 6) helps to delineate the distribution of West Antarctica's continental crustal terranes (Garrett et al., 1987; Golynsky & Aleshkova, 2000; Johnson, 1999; Maslanyj & Storey, 1990). These terranes include the Antarctic Peninsula, Ellsworth-Whitmore Mountains (EWM), the Filchner and Haag Nunataks, Marie Byrd Land, and Thurston Island (Ferraccioli et al., 2000, 2006; Golynsky & Aleshkova, 2000; Jordan et al., 2013; Luyendyk et al., 2003; Maslanyj et al., 1991). The thick sequences of Paleozoic sedimentary and metasedimentary rocks of the EWM are marked by a smooth magnetic anomaly field with superposed higher frequency anomaly maxima related to the Middle Jurassic plutonic complexes from the early break-up of Gondwana (Ferraccioli et al., 2000, 2006; Golynsky & Aleshkova, 2000; Jordan et al., 2013; Luyendyk et al., 2003;

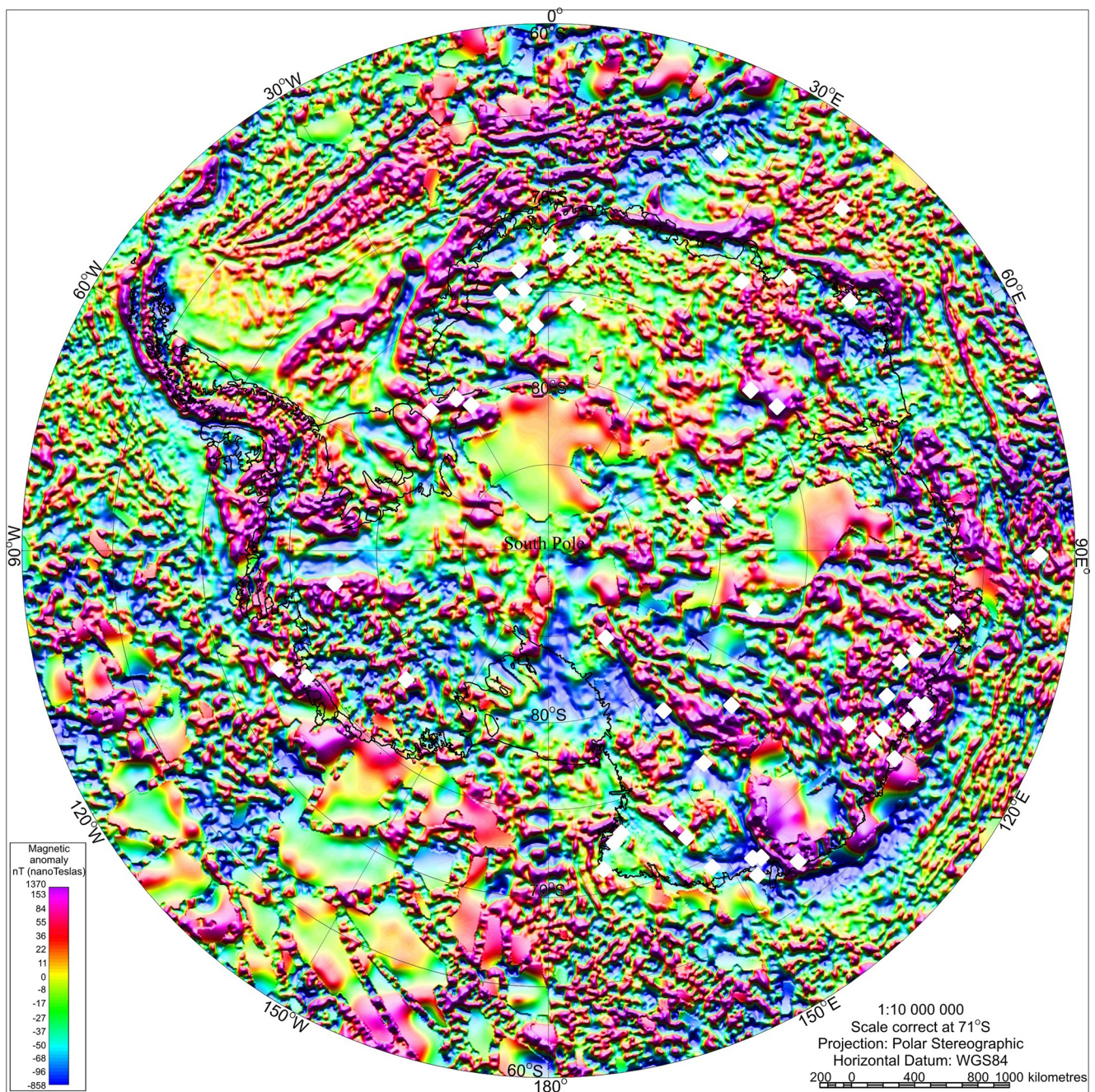


Figure 6. The Antarctic Digital Magnetic Anomaly Project's second-generation satellite-data supplemented map (ADMAP-2s) of near-surface scalar total field magnetic anomalies derived from the gap-filled grid of Figure 4 differentially upward continued to the Earth's mean geocentric radius of 6,371.2 km. The bold white-filled diamond symbols mark the cra coordinates from Figure 4 as numerically annotated in the text and Figure 5.

Maslanyj et al., 1991). The elevation variations of these anomalies inferred from the maps in Figure 8 suggest that this anomaly field persists up through Swarm altitudes with the short-wavelength components severely attenuated.

In contrast, intense relatively lower frequency anomaly maxima trending predominantly NW/SE characterize the area of the Haag Nunataks and their possible extension beneath the Ronne Ice Shelf, the EWM, and southern Palmer Land (Golynsky & Aleshkova, 2000; Maslanyj & Storey, 1990). However, Figure 8 shows that these anomalies are strongly suppressed at altitudes of about 75 km and higher, and thus poorly imaged by the Swarm mission data.

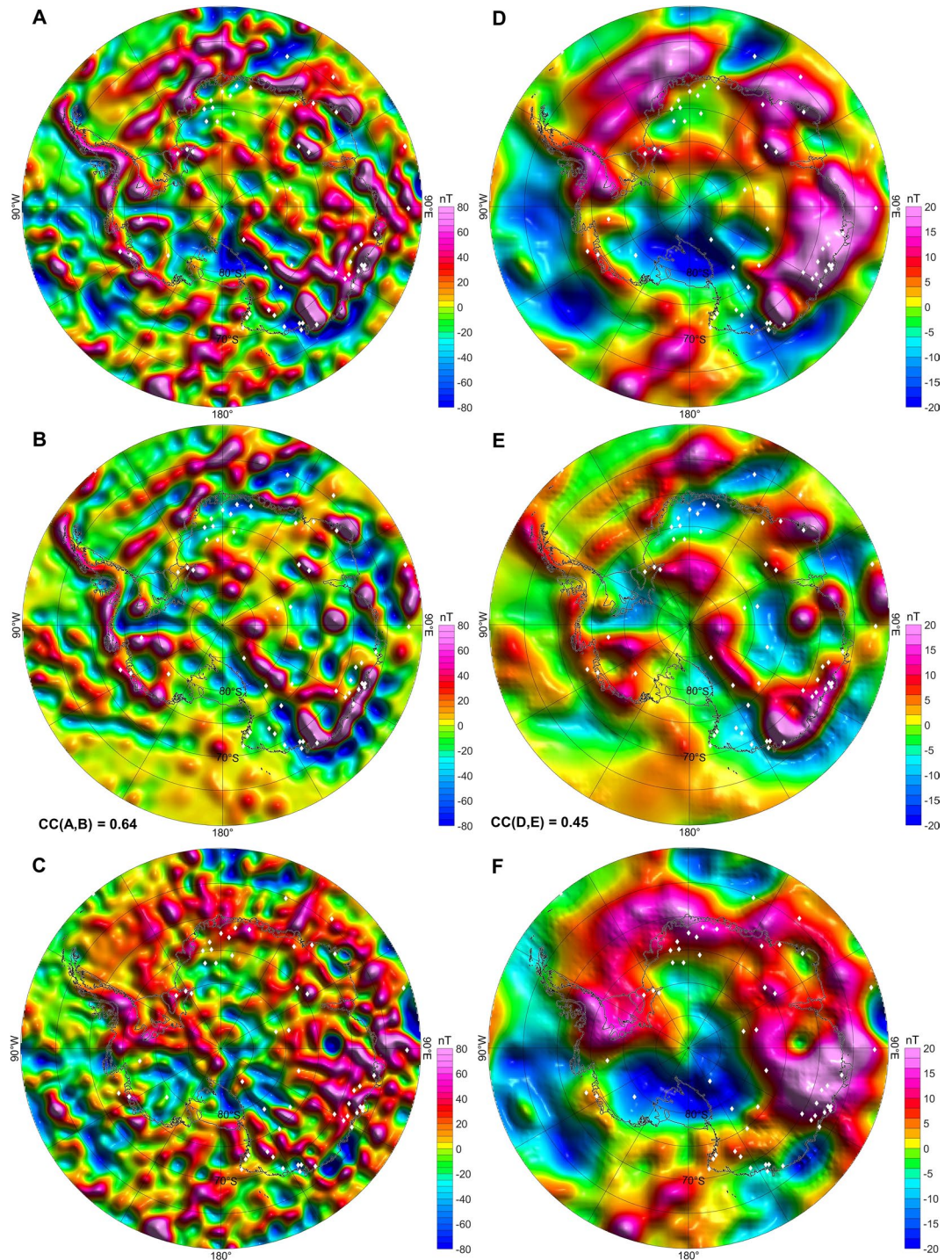


Figure 7. Total field magnetic anomaly comparisons of the Antarctic Digital Magnetic Anomaly Project-2s near-surface regional anomaly grid (Map **A**) with the downward continued Swarm magnetic anomaly estimates (Map **B**) at the Earth's mean geocentric radius of 6,371.2 km, and their (Map **A** – Map **B**) - differences (Map **C**), as well as the EPS upward continued ADMAP-2s near-surface anomalies (Map **D**) with Swarm's magnetic anomalies (Map **E**) at 250 km above the Earth's mean geocentric radius, and their (Map **E** – Map **D**) - differences (Map **F**). The correlation coefficients between the anomaly maps are also posted. The bold white-filled diamond symbols in the maps mark the cra coordinates from Figure 4 as numerically annotated in the text and Figure 5.

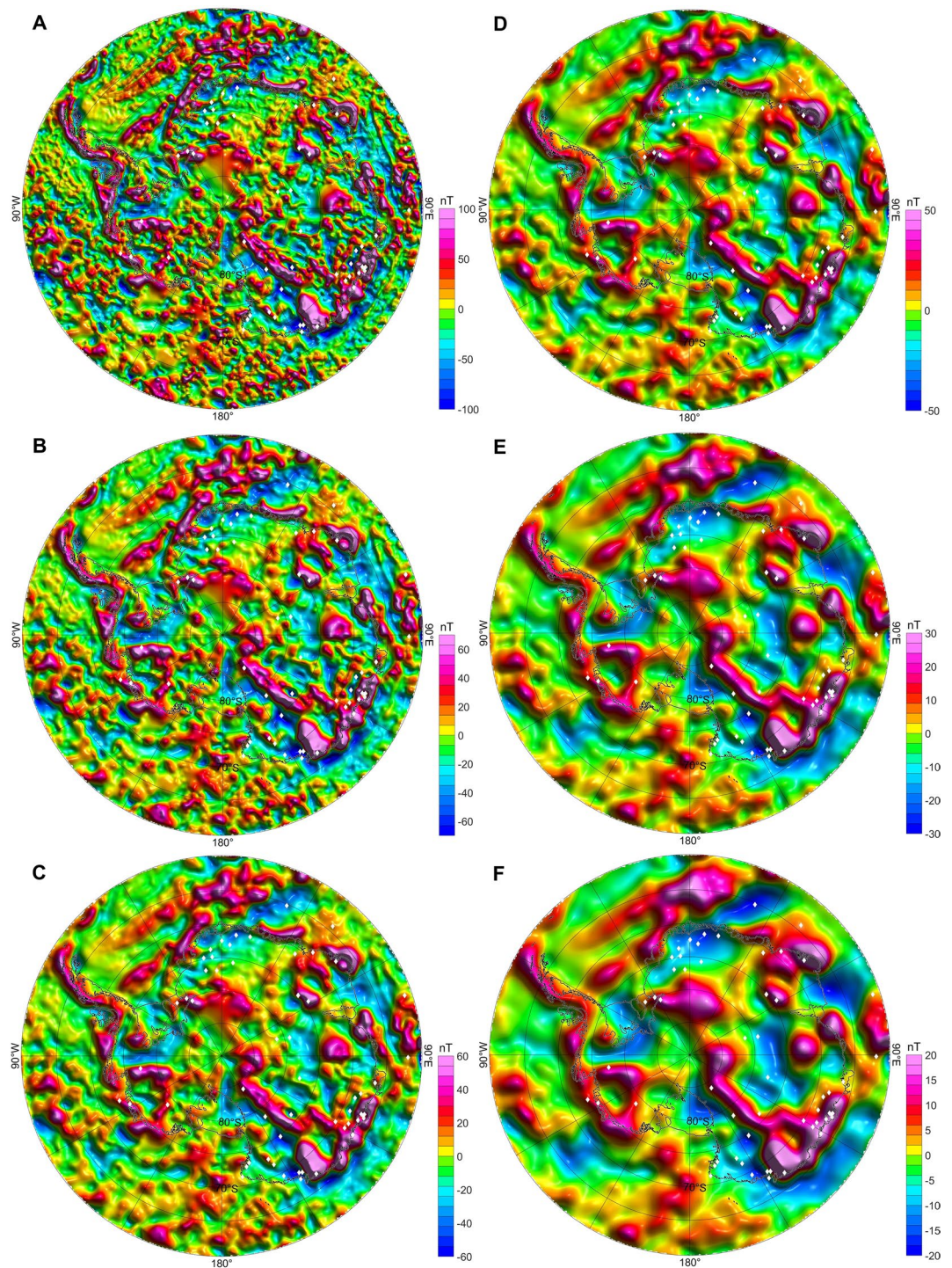


Figure 8. Antarctic scalar total field magnetic anomaly estimates over the geocentric altitudes of (a) 25 km, (b) 50 km, (c) 75 km, (d) 100 km, (e) 150 km, and (f) 200 km above the Earth's mean radius of 6,371.2 km. The bold white-filled diamond symbols in the maps mark the cra coordinates from Figure 4 as numerically annotated in the text and Figure 5.

The West Antarctic Rift System (WARS) forms one of the largest continental rift systems on Earth. It extends from the Amundsen Sea Embayment (ASE) along the eastern margin of the TAM to the Ross Sea. Here, widely spaced reconnaissance aeromagnetic profiles and detailed local surveys suggest the extensive presence of late Cenozoic volcanic rocks for the continental shelf and beneath the West Antarctic and Ross Sea Ice Sheets (Behrendt, 1964;

Behrendt et al., 1996; Jankowski et al., 1983). The shallowly buried volcanic rocks yield numerous short-wavelength, high-amplitude (100-to-1000+ nT) anomalies as the principal magnetic effect of the WARS. However, the 3-km Nyquist wavelength ADMAP-2 and -2s near-surface anomaly grids and their upward continuations represent this effect only marginally.

Much like the better-known Ross Sea segment of the WARS (Behrendt, 1999), both the Cretaceous rifting related to the separation of New Zealand from West Antarctica (Gohl et al., 2013) and the subsequent WARS-affiliated narrow-mode Cenozoic rifting (Bingham et al., 2012; Jordan et al., 2010; Smith et al., 2013) affected the ASE's development. Within the ASE, the cluster of positive aeromagnetic anomalies centered roughly at (cra) coordinates [72.97°S, 113.64°W] suggests the presence of widespread Neogene igneous rocks between the outcrops of the Hudson Mountains and the deep interior of the Pine Island Glacier (PIG) catchment and Marie Byrd Land Dome. These rocks may be related to the narrow rift basins west of 98°W (Young et al., 2017), whereas further east, the anomalies suggest weakly magmatic WARS basins that may skirt the EWM.

In this study, the cra-coordinates are numbered according to the order in which they are called out in the text. Thus, cra1[72.97°S, 113.64°W] denotes the above first called out set of cra coordinates, which a bold solid white diamond symbol also marks in Figure 4 and other magnetic anomaly maps. Figure 5 also enumerates the bold solid white diamond symbols for all 58 cra-coordinates called out in the text.

The prominent regionally positive N/S-trending magnetic anomaly belt cra2 [77.43°S, 98.77°W] in Figure 4 presumably relates to the enhanced magmatism during Cretaceous New Zealand–Antarctic rifting and breakup at ca. 90 Ma (Gohl et al., 2013) or the possible development of one or more narrow rift-basins along the edge of the EWM (Bingham et al., 2012; Jordan et al., 2010; Smith et al., 2013). The origins of the less distinct, weaker more curvilinear and broken up western anomaly belt cra3 [78.84°S, 132.13°W] are not well understood. However, it may reflect the effects of pre-breakup arc-related magmatism, or perhaps the break-up events involving the Cenozoic magmatism from the mantle plume beneath the Marie Byrd Land dome. The western belt along roughly 135°W bisects the dome where the underlying mantle plume may be driving ongoing alkalic volcanism (e.g., Mukasa & Dalziel, 2000).

Continental rifting and magmatic processes presumably elevated heat flow at both local and regional scales, thereby increasing the availability of water at the base of the ice sheet. The aeromagnetic data reveal subglacial sedimentary basins in the ASE that may have further enhanced glacial flow (Bingham et al., 2012; Jordan et al., 2010; Smith et al., 2013).

North of the WARS, the new Antarctic Peninsula aeromagnetic data are helping to decipher Mesozoic arc magmatism and crustal terrane accretion along Gondwana's paleo-Pacific active margin (Ferraccioli et al., 2006; Ghidella et al., 2013; Gohl et al., 2013; Jordan et al., 2014). These studies suggest that a 1,500+ km shear zone running along the Antarctic Peninsula batholith may mark the collisional suture between a seaward mafic arc and a landward felsic arc at the active margin during the Cretaceous Palmer Land event (Ferraccioli et al., 2006; Vaughan et al., 2012). Accordingly, this event saw intrusions of highly magnetic tonalitic/granodioritic island arc plutons in the crust, in contrast to long-lived in situ magmatism that offers an alternate interpretation (Burton-Johnson & Riley, 2015). West of the Antarctic Peninsula across Adelaide Island (AI), high resolution aeromagnetic surveying maps the extent of Cenozoic magmatism along the arc/forearc boundary. Here, about 25% of the upper crust consists of Paleogene and Neogene plutons to highlight the complexity and longevity of its magma emplacement. Accordingly, source interpretations vary for the prominent magnetic Pacific Margin Anomaly (PMA—Figure 4), which runs the length of the Antarctic Peninsula from Thurston Island to the South Orkney Microcontinent (Jordan et al., 2014; Maslanyj & Storey, 1990). However, the magnetic anomalies for the Antarctic Peninsula and South Orkney Microcontinent are well-defined up through Swarm altitudes to suggest regionally pervasive enhancement of the crust's magnetization.

Over the Möller and Institute ice streams, the new N/NW-trending positive aeromagnetic anomalies map out crustal features of the Weddell Sea Rift along the EWM's eastern margin. They include the effects of the rift's pre-existing Proterozoic basement and Middle Cambrian volcanic rocks, Jurassic intrusions, and the presumed post-Jurassic sedimentary rocks beneath the ice. The rift's kinematics suggest it formed between East and West Antarctica along part of a major left-lateral strike slip fault (Jordan et al., 2013). This boundary appears not only to have focused emplacements of the Jurassic intrusions, but also may have accommodated the displacement of

the EWM southwards at the beginning of Gondwana's break-up. However, the related magnetic anomalies fade quickly with altitude and are poorly imaged by the Swarm data.

3.2. East Antarctic Magnetic Anomalies

This section summarizes possible crustal geology-magnetic anomaly associations for several sectors that connect to cover East Antarctica. Each sector radiates from the South Pole over the broad longitude limits described below.

3.2.1. Dronning Maud Land Sector

This sector of western East Antarctica extending to roughly 40°E includes a well-defined E/W band of the near-surface magnetic anomalies in western Dronning Maud Land (DML) that may mark the East Antarctic Shield's margin (Golynsky & Aleshkova, 2000; Riedel et al., 2013). The broad low-gradient magnetic minimum interspersed with linear weak magnetic anomaly maxima delineates the extent of the Archean-to-Mid-Proterozoic Grunehogna Province (GP in Figure 4) as a likely fragment of Africa's Zimbabwe-Kaapvaal Craton (Groenewald et al., 1991). The ca. 1.1 Ga magmatic rocks of the Namaqua-Natal-Maud Belt (or Maudheim Province; Groenewald et al., 1991) that rims the craton's fragment are marked by elongated, high-amplitude positive magnetic anomalies. The anomaly features for both the Grunehogna and Maudheim Provinces broadly transform with altitude into a regional anomaly minimum surrounded by a ring of maxima, which to the west along the coastline represent a prominent segment of the Maud Belt (Figure 8).

Within the western Maud belt of magnetic anomalies (MBMA in Figure 4), the Heimefront lineament magnetic anomaly (HLMA in Figure 4) is a major magnetic discontinuity that overlies the Heimefront Shear Zone, which may control the magnetic contrasts more structurally than lithologically (Golynsky & Jacobs, 2001). Northwest of the HLMA, broad, elongate, and high amplitude positive anomalies may map the edge of the Grenvillian cratonic rim. Southeast of the HLMA, the Grenvillian crust exhibits a broad magnetic minimum $cra4$ [74.82°S, 10.34°W], which is overprinted by smaller anomalies trending mostly NW along the Pan-African structural trend identified for the Sivorg Terrane of the Heimefrontfjella (HF; Jacobs et al., 1996). Thus, the HLMA may delineate a crustal-scale feature separating overprinted Mesoproterozoic Pan-African crust in the east from Pan-African crust in the west (Jacobs et al., 1996). Specifically, it may mark the East African-Antarctic orogen's western front that is broadly contemporaneous with and structurally orthogonal to the Ross Orogen in the TAM (Kleinschmidt & Buggisch, 1994; Tessensohn, 1997). Further northeastwards at the Midbresrabben Hills, a network of some 400-m wide anastomosing mylonitic shear and cataclastic zones cut across banded gneisses like those of the H.U. Sverdrupfjella (HUS)'s basement (Grantham & Hunter, 1991). Accordingly, the Heimefront Shear Zone appears to be a major crustal-scale structure that continues for at least another 250 km as the western boundary of the East African–Antarctic Orogen (Jacobs & Thomas, 2004).

The MBMA's southern boundary lacks outcrop constraints, but south of HF, the aeromagnetic data transition from a series of moderate amplitude elongate minima and maxima into sharply contrasting, isolated shorter wavelength anomalies over the Coats Land Block (CLB; Golynsky & Aleshkova, 2000; Mieth & Jokat, 2014). The buried basement of the CLB is possibly a sliver of Laurentia within Rodinia (Gose et al., 1997; Loewy et al., 2011) resulting from Archean-to-early Mesoproterozoic tectonism (Golynsky & Aleshkova, 2000; Jacobs et al., 2003). Its dome-like morphology and magnetic anomalies portray it as perhaps a relatively stable Pre-Grenvillian buttress against the deformation of the surrounding mobile belts, where thermotectonic events strongly altered and magnetically imprinted its basement rocks.

Positive anomalies in Figures 7a and 7b, and 8a–8c Figures 7a and 7b, and 8a–8c partially ring the CLB's regional anomaly minimum with a weakly defined eastern boundary. At the higher altitudes in Figures 8d–8f, however, the irregularly shaped anomaly minimum just west of the Shirace Glacier (ShG) with elements $cra5$ [76.72°S, 10.51°W] and $cra6$ [70.88°S, 35.69°E] appears to map the extent of the Grenville collisional orogenesis during the late Neoproterozoic-to-Early Cambrian.

The southern margin of the CLB features an elongate regional maximum $cra7$ [79.67°S, 31.34°W] over the Shackleton Range crustal block (SRCB). Positive anomalies of amplitudes up to 500 nT characterize the SRCB in contrast to the CLB's relatively subdued magnetic signature (Golynsky & Aleshkova, 2000). Outcrop studies show that the SRCB consists of basement rocks from the Precambrian Stratton and Pioneers Groups which

underlie Neoproterozoic sedimentary rocks. The basement groups sustained strong thermotectonic overprinting at ca. 500 Ma and were thrust over the Paleoproterozoic Read basement that was not overprinted during the lower Paleozoic (Tessensohn, 1997).

In the Shackleton Range (SR), Neoproterozoic sedimentary rocks in association with ca. 500 Ma ophiolitic outcrops and high-pressure evidence for metamorphism up to eclogite facies (Schmadicke & Will, 2006) support the CLB-bounding presence of a late Neoproterozoic/early Paleozoic suture zone. Talarico et al. (1999) and Kleinschmidt et al. (2002) suggest the suture developed by closure of an ocean in sinistral transpression. The ocean, in turn, may have lain off the East African-Antarctic Orogen's eastern margin, or perhaps at the northern margin of the Mawson Continent (Will et al., 2010). Despite the presence in outcrop of ophiolite rocks with large magnetic susceptibilities (e.g., $[59.0\text{--}350] \times 10^{-3}$ SI; Sergeev et al., 1999), neither of the inferred continuations of the suture is marked by the continuation of the prominent magnetic anomalies. Instead, the continuous belt of E/W-trending, high-intensity magnetic anomalies cra8 [80.26°S, 8.95°E] extends from the SR into East Antarctica for at least 500 km where the belt's orientation roughly changes to a N/S-trend in the Recovery Lakes (RL) region (Ferraccioli et al., 2016). Figure 8 illustrates the eastward continuity of the linear belt, although the Swarm observations do not appear to resolve the RL's N/S-trending component.

To the west, the SR's mostly E/W-trending magnetic maxima cra9 [79.39°S, 40.18°W] terminate at the margin of the Weddell Sea Embayment. Comparable linear magnetic maxima over the Haag Nunatak crustal block may be reconstructed into continuity with the SR anomalies by undoing Jurassic crustal extension in the embayment (Jordan et al., 2017). Accordingly, despite the presence and lack of Paleozoic sediments in the respective SR and Haag Nunataks outcrops, this reconstructed mobile belt may have been active from the Proterozoic to the early Paleozoic (Golynsky, 2007; Jordan et al., 2017). The SR's magnetic maxima appear to involve relatively superficial enhancements of crustal magnetization given that they attenuate quickly with altitude in the anomaly continuations of Figure 8.

The mountains of central DML are marked by a regional low-amplitude minimum cra10 [71.48°S, 6.88°E] interspersed with high-frequency maxima (Damaske, 1999; Golynsky et al., 2001; Mieth & Jokat, 2014; Riedel et al., 2013). By Figure 8, the minimum anomaly persists up through Swam altitudes, whereas the shorter wavelength maxima reflect more superficial crustal magnetization effects that quickly attenuate with altitude. Most of the local maxima are associated with voluminous and mainly undeformed Pan-African post-tectonic granitoids. The coastal outcrops all indicate Grenville basement that suffered Pan-African reworking to varying degree (Jacobs et al., 1998; Shiraishi et al., 1994).

South of the DML mountains, a smooth low amplitude minimum anomaly province cra11 [73.01°S, 4.29°E] terminates the 400 km long and 65 km wide Forster Magnetic Anomaly (FMA in Figure 4). Consisting of segmented linear SW/NE-trending anomalies (Riedel et al., 2013), the FMA may mark the edge of a major tectonic block and/or a suture zone within the East African-Antarctic Orogen (Jacobs & Thomas, 2004; Riedel et al., 2013). However, the FMA is severely suppressed at the higher altitudes in Figure 8 so that its interpretation for the effects of a major crustal magnetization's edge and/or a suture zone seems dubious.

The FMA also may be an eastward continuation of a linear anomaly cra12 [74.83°S, 5.40°W] located southward of the Grenvillian/Kibaran orogeny-affiliated Sverdrupfjella-Kirwanveggen Anomaly with elements cra13 [73.68°S, 6.02°W] and cra14 [72.44°S, 0.14°E] (Golynsky & Aleshkova, 2000). The underlying crustal province may represent an older cratonic block or the southern foreland extension of the western Rayner Complex (Jacobs et al., 2015). The region SE of the FMA involves sinuous, SE-trending magnetic highs of moderate intensities (Mieth & Jokat, 2014). Complementary outcrop, geochronological, and geochemical data suggest that the anomaly maxima may reflect the effects of juvenile Tonian crust formed in oceanic accretionary settings. However, this Tonian Oceanic Arc Superterrane (TOAST) lacks strong metamorphic overprint and has minimal Rodinia affinity (Jacobs et al., 2015) and magnetic effects at Swarm altitudes (Figure 8).

In southern DML around the Valkyrie Dome ice feature, the new aeromagnetic data show a prominent curvilinear belt of segmented positive magnetic anomalies (Forsberg et al., 2018; Mieth & Jokat, 2014). This anomaly belt with elements cra15 [75.67°S, 6.92°E] and cra16 [76.92°S, 3.33°W] may outline the Valkyrie Cratonic Block (VCB in Figure 4; Golynsky, 2007; Golynsky et al., 2018). In Figure 4, the VCB's northern and western boundaries appear to be outlined by narrow anomaly maxima, whereas broader, higher amplitude maxima mark its southern and eastern boundaries. ADMAP-2 and newer data (Ruppel et al., 2018) reveal the anomaly belt to

be relatively continuous and encompassing predominantly low-amplitude regional minima that may be affiliated with back-arc sedimentary basins sandwiched between the TOAST and the Valkyrie craton.

3.2.2. Enderby Land-To-Princess Elizabeth Land Sector

This sector of East Antarctica from roughly 30°E to 90°E includes the Enderby Land, MacRobertson Land, Princess Elizabeth Land (PEL), and the Prince Charles and subglacial Gamburtsev Mountains. In Enderby Land, the roughly oval belt of anomaly maxima cra17 [67.50°S, 50.38°E] differentiates the Archean Napier Complex from the negative magnetic signature of the Mesoproterozoic Rayner Complex to the south that continues toward MacRobertson Land (ML; Golynsky, Morris, et al., 2002). This belt, together with the magnetic anomalies of the northern Prince Charles Mountains (PCM) and the neighboring eastern Lambert Rift shoulder (Ravich et al., 1985), runs from the Prince Olav Coast (POC) toward PEL to mark a wide continental-scale accretionary orogen (i.e., the Rayner continental arc). This feature is also partly preserved in India (Mezger & Cosca, 1999) and may date to ca. 990–920 Ma (Mikhalsky et al., 2015). However, in Figure 8, it quickly fades with altitude and thus is poorly resolved in the Swarm anomalies.

Also fading rapidly with altitude is the prominent positive 350-nT amplitude anomaly cra18 [69.03°S, 41.36°E] that marks the boundary between the Rayner Complex and the Lützow-Holm Bay Complex (LHBC) to the west (Golynsky et al., 1996; Nogi et al., 2013). The fragmented E/W-trending magnetic maxima and minima of the LHBC reflect the effects of rocks subjected to granulite facies metamorphism. The westward changing magnetic anomaly pattern persists up to Swarm altitudes in Figure 8 to mark the boundary between the LHBC and the neighboring Yamato-Belgica Complex (Golynsky et al., 1996).

Figure 9 exemplifies how the aeromagnetic anomalies for the PCM and surrounding areas may be used to infer a complex, but coherent first-order interpretation of the region's crustal geology and tectonic history (Golynsky, Golynsky, et al., 2006; Golynsky, Masolov, et al., 2006). Magnetic anomaly correlations with known geologic features and trends allow for regional-scale geological mapping of ice-covered regions and differentiating magnetic crustal subdivisions like the Vestfold [1a, 1b], Rayner [2], PEL [3], and Ruker [4] terranes. For example, intense positive anomalies [1a, 1b] associated with Late Archean high-grade metamorphic rocks encompass the Vestfold Hills (VH) and Rauer Islands to suggest a crustal block marked by a regional oval anomaly maximum that persists up to Swarm altitudes in Figure 8. However, the predominantly NE-trending magnetic fabric of the northern PCM that can be traced to the Lambert Rift's eastern margin rapidly fades out with altitude in Figure 8. This fabric's minima correlate with the Athos supracrustals [2a] and its maxima mostly map the Beaver Complex's Porthos orthogneisses [2b] and charnockite-granulite terrane (Kamenev et al., 1993). Moderate amplitude banded anomalies characterize the Mesoproterozoic Fisher Complex's [2 d] diverse juvenile volcanics from ca. 1,400–1,200 Ma (Mikhalsky et al., 2013), whereas the calc-alkaline components suggest an island arc setting (Mikhalsky et al., 1996).

A prominent linear system of alternating anomalies trending NE/SW at the Lambert Rift's eastern shoulder is associated with the predominantly orthogneissic Pickering Series [3] and paragneissic Manning Series [3a] (Golynsky & Golynsky, 2007; Laiba & Kudriavtsev, 2006). Figure 8 suggests that this anomaly trend is perceptible as linearly continuous minima up to about 75 km altitude. From the U-Pb zircon ages and chemical compositions, the rocks are essentially the same as those of the Beaver Complex (Mikhalsky et al., 2013), although the magnetic anomaly attributes for the two regions differ (Golynsky, Masolov, et al., 2006). The mafic granulites of the Manning Nunataks (MN) can be related to metamorphosed island arc basalts, whereas the relationship of the felsic volcanic arc orthogneisses to subduction of oceanic crust remains enigmatic (Liu et al., 2014). Protolith ages range from ca. 1,347 to 1,020 Ma to suggest a long-lived site of crustal accretion for the Rayner continental arc. Thus, aeromagnetic surveying of PEL [3] has imaged a unique Stenian-aged accretional orogen in East Antarctica (Liu et al., 2016; Mikhalsky et al., 2015). The orogen can be traced from the Clemence Massif in the central Lambert Glacier [LG] to the southern margin of the VH and further eastwards to 88°E (Golynsky et al., 2018).

Located largely over the eastern Amery Ice Shelf coast, the prominent Robertson Magnetic Anomaly (RoMA in Figure 4 & [3c] in Figure 9; Golynsky, Masolov, et al., 2006) seems to be suppressed at Swarm altitudes as shown in Figure 8. It appears to reflect the effects of amphibolite-facies rocks that only outcrop in the Robertson Nunatak (RN) as migmatitic mafic schists and subordinate Bt-Pl orthogneiss (Laiba & Kudriavtsev, 2006; Mikhalsky et al., 2013). These isotopically juvenile rocks, together with those of the Fisher Terrane, may represent the

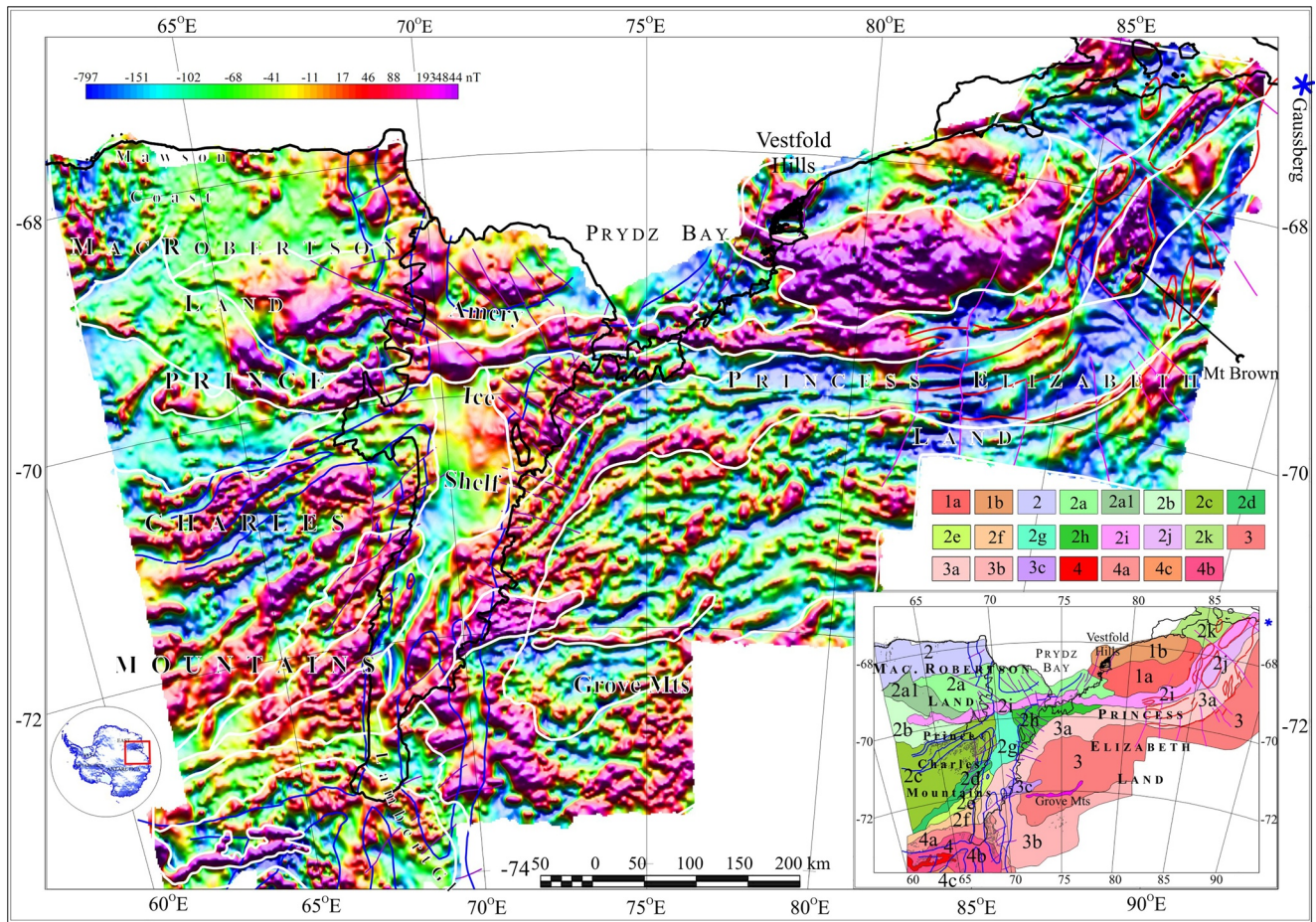


Figure 9. Crustal magnetic anomalies of MacRobertson Land and Princess Elizabeth Land from Russian airborne surveys. White lines roughly delineate crustal subdivisions inferred from the first-order variations in anomaly amplitudes and gradients. The bottom-right insert generalizes the distribution of the subdivisions and the text gives additional information on their possible geological implications. Heavy blue and red lines delineate the Lambert and Gausberg rifts (Golynsky & Golynsky, 2007), respectively. Lines of other colors infer faults, lineaments, and other structures. The blue asterisk at the upper right of the study region locates the Gausberg volcano.

remnants of an oceanic arc that the Lambert Rift separates by some 50–60 km of dextral displacement. It may be attributed to oblique or strike-slip faulting during the opening of the rift, and thus may be related to the Mesozoic break-up of India and East Antarctica. Dextral strike-slip faults also dissect the Permo-Triassic Amery Group in the northern PCM (Boger & Wilson, 2003) and offset metamorphic isograds southwards by a few tens of kilometers (Kamenev et al., 1993).

The Archean Ruker Complex (RC in Figure 4) of metamorphic rocks is mainly expressed by low-amplitude positive anomalies within a regional negative anomaly. The anomaly maxima reflect the effects of metamorphosed granite-gneiss basement rocks that experienced major early Precambrian (ca. 3,500–2,100 Ma) tectono-magmatism. Within the southern PCM, the Ruker Magnetic Anomaly (RMA in Figure 4 and [4] in Figure 9) is a prominent magnetic lineament associated with a banded iron formation (Golynsky, Alyavdin, et al., 2002). Russian reconnaissance surveying has obtained evidence for possibly extending the RMA westward some 120 km (Golynsky, Alyavdin, et al., 2002). However, in Figure 8, the RMA fades quickly with altitude, and thus is poorly resolved in the Swarm anomalies.

The elongate near-surface magnetic minimum cra19 [79.19°S, 74.91°E] appears to mark a major collisional suture that separates the Archean RC from the Proterozoic Gamburtsev Mountains Province (Ferraccioli et al., 2011). However, the timing of the final assembly of central East Antarctica along this and other sutures remains controversial due to the lack of outcrops. Using ADMAP-1 data, Golynsky (2007) offered an alternative by which the GMP may contain several sub-provinces where the suture possibly forms the southern boundary of a

Mesoproterozoic orogenic belt that encompasses the RC. The putative magnetic anomaly belt also may represent the extension of the TOAST that formed in central DML near the margin of the Rodinia supercontinent (Jacobs et al., 2015).

Prominent positive near-surface magnetic anomalies mark the Gamburtsev Mountains Province cra20 [81.14°S, 73.04°E] that may form a continuous curvilinear belt with the SR maxima cra21 [80.43°S, 28.03°W], although the paucity of the available aeromagnetic data may somewhat limit the veracity of this association. In the Swarm observations, arcuate maxima mark the RC's northern and southern boundaries where isolated anomaly minima surround the relatively subdued central Mellor Anomaly (Golynsky, Alyavdin, et al., 2002) with positive elements cra22 [74.36°S, 57.81°E] and cra23 [75.06°S, 51.57°E].

3.2.3. Queen Mary Land-To-Adélie Land Sector

This sector extends roughly from 90°E to roughly 145°E and covers Queen Mary Land, Lake Vostok, Wilkes Land, and Adélie Land. The near-surface grid coverage (Figure 4) for Wilkes Land incorporates new aeromagnetic data from the campaign abbreviated Investigating the Cryospheric Evolution of the Central Antarctic Plate (Blankenship et al., 2011). These data help to resolve Gondwana's crustal structures to constrain the Mesoproterozoic reconstruction of Australia and Antarctica (Aitken et al., 2014, 2016). Southern Australia's crustal features that may extend beneath the East Antarctic Ice Sheet include the East and West Mawson cratons, the Charcot, Vestfold, Vostok and Gamburtsev-Ruker-PEL terranes, the Albany-Fraser Province, the Aurora, Conger, Frost, Scott and Totten transcontinental faults, as well as the Indo-Australo-Antarctic suture (IAAS) that arguably trends S/SE from Scott Glacier inland some 1,500 km or more (Aitken et al., 2014).

The IAAS is marked by the along-strike changes in aeromagnetic anomaly amplitudes, frequencies, patterns and other attributes that suggest its intersection with the coast near the Scott Glacier ($\approx 100.5^\circ\text{E}$) and southward extension past Lake Vostok (Studinger et al., 2003). However, Gardner et al. (2015) argued that crustal rifting may have displaced the IAAS some 50 km westwards to near the Denman Glacier ($\sim 99.5^\circ\text{E}$), whereas Maritati et al. (2016) suggested that the IAAS may also pass through Chugunov Island some 100 km off the coast.

To constrain the Indo-Australo-Antarctic boundary across Gondwana from NE India past Mirny Station into East Antarctica (Daczko et al., 2018), analyzed detrital zircons from offshore East Antarctica between 60°E and 130°E together with complementary terrestrial U-Pb geochronology and geophysical data (Mulder et al., 2019). They argued that the India-Australia paleo-plate boundary may intersect East Antarctica's coast near roughly 94°E as a subglacial fault, which Aitken et al. (2014) inferred from widely spaced ICECAP profiles and Daczko et al. (2018) called the Mirny Fault. However, new detailed bedrock topography and aeromagnetic anomaly data that Russian surveys collected recently east of the Mirny Station do not appear to observe this fault (Golynsky, Golynsky, & Kiselev, 2021, in preparation) so that the crustal attributes of the IAAS remain enigmatic.

In general, the ICECAP aeromagnetic data-based elements of the near-surface anomaly grid may be broadly considered in terms of their features over central Wilkes Land between the Denman Glacier and the Clarie Coast (136.2°E), Adélie Land, Lake Vostok, and the Queen Mary Coast. Within central Wilkes Land, the magnetic province includes several linear anomaly belts that run roughly E/W over the Law Dome area and the nearby Totten Glacier axis cra24 [67.15°S, 115.27°E]. Further southwards, the curvilinear anomaly belts convex northwards, where the most intense anomaly maxima with amplitudes up to 1,500 nT overlie the Law Dome and neighboring areas. Also, the strongest negative anomaly here has an amplitude falling to -2150 nT. The anomaly belts may represent magnetic effects that are analogous to those of southwestern Australia's Albany Fraser Orogen (Aitken et al., 2014). In the southern reaches of these anomaly belts, Maritati et al. (2019) adjusted Aitken et al. (2014)'s ENE/WSW-trending aeromagnetic data lineament to intersect the coast in the vicinity of Chick Island cra25 [66.79°S, 121.0°E]. They inferred the modified magnetic lineament to mark the Southard Fault between their named Banzare and Nuyina crustal provinces that, in turn, may be the Antarctic conjugates of Australia's Coompana and Madura provinces, respectively.

Continuing south of the Totten Glacier, negative anomalies cra26 [68.74°S, 107.46°E], cra27 [68.77°S, 113.24°E], and cra28 [68.35°S, 120.32°E] predominate, where the belt's eastern part cra29 [68.16°S, 118.06°E] may involve the positive and negative magnetic effects of respectively uplifted and subsided crustal blocks. The width of this belt is about 140 km in its central and eastern parts, whereas it appears to die out to the west in the Aurora Subglacial Basin area cra30 [68.11°S, 105.16°E]. Between the IAAS and Aurora fault, the near-surface magnetic anomalies of Aitken et al. (2014) change from roughly E/W to N/S trends due possibly to the overprinting effects of the

paired rift system underlying the Scott Glacier's southern extension and the Aurora Subglacial Basin, where Late Paleozoic–Triassic intracontinental extension produced the intervening highlands (Golynsky & Golynsky, 2012). Figure 8 shows that the related anomaly minimum is well-defined from near-surface through Swarm altitudes.

The Adélie Land's magnetic province is associated with Australia's Mawson Craton (Aitken et al., 2014; Fanning et al., 1995). It contains the Archean-to-Paleoproterozoic rocks that are also found along the George V coast which have geological affinities with the Gawler Craton's rocks in southern Australia. This province lacks magnetic profiles through its largest central part and thus is poorly surveyed. However, thin elongated anomalies with NNE/SSW trends map both the western and eastern margins of the Mawson Craton relatively well. The linear anomaly belts roughly terminate along 85.5°S between 157°E and 135°E to possibly delineate the Mawson Craton's southernmost boundary. Swarm anomaly maxima mark the eastern boundary of the Mawson Craton, but its western margin is relatively poorly defined in the satellite magnetic data.

In our near-surface anomaly grid, the Lake Vostok magnetic province does not appear to extend to the Knox rift cra31 [66.3°S, 100.0°E] as Aitken et al. (2014) proposed. This province contains mostly elongate positive anomalies of moderate amplitudes along the eastern coast and the southern end of Lake Vostok cra32 [75.6°S, 106.0°E]. The Lake Vostok magnetic province generally shows low-amplitude short-wavelength anomalies in a negative regional background that seems to be poorly expressed in the Swarm data.

The Queen Mary Land magnetic province over the Charcot terrane west of the Denman Glacier area involves a sparse network of profiles (Aitken et al., 2014). The related poorly constrained components of the near-surface anomaly grid are dominated by low-amplitude, short-wavelength anomalies. However, this magnetic province is also poorly resolved in the Swarm data to suggest that it involves mostly superficial crustal magnetizations with effects that rapidly attenuate with increasing altitudes.

Northern Wilkes Land features numerous near-surface magnetic anomaly maxima that integrate with altitude in Figure 8 into the largest amplitude Swarm anomaly maximum of the Antarctic that the Magsat, Ørsted, and CHAMP satellite magnetometers have also mapped (von Frese et al., 2013). They overlie crust that possibly extends into southcentral Australia, where the enhanced crustal magnetization may involve magmatic contributions from giant meteorite impact in a normal-polarity geomagnetic field at ca. 260 Ma and the subsequent Mesoproterozoic rifting of Australia from East Antarctica (Kim & von Frese, 2017; von Frese et al., 2009; Zhang et al., 2020). The inferred impact also may have produced the putative 500-km diameter Wilkes Land subglacial meteorite basin cra33 [70°S, 120°E] in Figures 1 and 2, and triggered the end-of-Permian activation of the antipodal Siberian traps and the Earth's greatest mass extinction.

3.2.4. George V Coast-To-Victoria Land Sector

This sector extends from roughly 145°E to the eastern margin of East Antarctica along the TAM. The near-surface grid coverage in Figure 4 also includes aeromagnetic data contributions from international surveys that jointly obtained sub-ice radar and aerogravity observations for the Wilkes Subglacial Basin (WSB) and TAM to help investigate the crustal architecture and geology at East Antarctica's eastern margin (Ferraccioli et al., 2009, 2017; Jordan et al., 2013; Studinger et al., 2004). For example, in Victoria Land aeromagnetic anomalies infer how Jurassic regional tholeiitic magmatism may have affected Palaeozoic terranes of the Ross-Delamerian orogen, which was subsequently dissected by faulting at the West Antarctic rift's shoulder.

They also constrain the transition between the Ross-aged terranes and the Precambrian interior of East Antarctica (Blankenship et al., 1993; Bosum et al., 1989; Damaske et al., 1994; Ferraccioli & Bozzo, 1999). For instance, strong aeromagnetic anomaly maxima (>500 nT) map the Cenozoic rift-related Meander Intrusives in the Malta Plateau (MP) region (Ferraccioli et al., 2009), whereas Jurassic-age Ferrar Group rocks are imaged in the Manning Nunataks (MN) region. Additionally, elongate short-wavelength magnetic maxima (100–200 nT) in the central TAM characterize the regional effects of Jurassic tholeiitic magmatism (Goodge & Finn, 2010) associated mostly with the Ferrar diabase dikes and sills. These features exhibit typical magnetic susceptibilities of about 8×10^{-3} SI or less as measured from outcrops throughout the TAM (Damaske & Finn, 1996; Ferraccioli & Bozzo, 1999; Goodge & Finn, 2010). In general, the near-surface anomalies fade rapidly with altitude, and thus are largely suppressed at Swarm altitudes.

Positive aeromagnetic anomalies over northern Victoria Land and southeastern Australia suggest that during the Ross-Delamerian orogeny, subduction-related plutons intruded the early Paleozoic margin of Gondwana (Finn

et al., 1999). These plutons in the respective conjugate Glenelg and Wilson terranes of Australia and Victoria Land may have formed magmatic arcs along the continental-margin. This magmatism's eastward migration culminated in the Stavely (Australia) and conjugate Bowers (northern Victoria Land) forearc volcanism. The Stawell (Australia) and conjugate Robertson Bay (northern Victoria Land) turbidites from the respective Glenelg and Wilson terranes were deposited onto the subducting oceanic plate. During the Delamerian and Ross orogenies, thrust faults truncated and uplifted the margin (Finn et al., 1999). The regionally positive aeromagnetic anomalies marking possible Paleozoic plutons within Northern Victoria Land persist up to Swarm altitudes (Figure 8) to suggest their pervasive and/or deep-seated crustal origins.

Along the WSB's eastern margin, the NW/SE-trending, roughly 300 km long aeromagnetic anomaly maximum may reflect the magnetic effects of Ross-age magmatic arc intrusions (Ferraccioli et al., 2009). The broad magnetic low between 156°E and 150°E exhibits superposed short-wavelength maxima that are comparable to the superposed maxima of the dominant broad magnetic high between 150°E and 144°E. These high-frequency magnetic anomalies within the WSB that overlie mesa subglacial topography may delineate Ferrar tholeiite intrusions of the Beacon Supergroup rocks during the Jurassic (Ferraccioli et al., 2009).

Modeling of combined airborne magnetic and gravity data suggests that WSB's central basins may be underlain by post-Jurassic grabens. These grabens appear to be analogous to the Rennick Graben and its neighboring elongate basins and the large fault-bounded troughs in Northern Victoria Land (Ferraccioli et al., 2009). The Matusevich Glacier (MG), for example, appears to be underlain by the ca. 480 Ma Exiles Thrust Fault System, which was reactivated by Cenozoic strike-slip faulting into northern Victoria Land roughly along the MG (Ferraccioli et al., 2002, 2003). Further to the west, the Prince Albert Fault System appears to control the WSB's eastern elongate basins (Ferraccioli & Bozzo, 2003). The aeromagnetic effects of the WSB in Figure 8 fade quickly with altitude, and thus are poorly resolved by the Swarm data.

For the Cook ice stream (CIS) glacial catchment cra34 [69.45°S, 152.63°E], the overlying near-surface regional magnetic minima suggest that the near-coastal basins may hold several kilometers of early Cambrian-to-late Neoproterozoic (?) sediments, which abut Proterozoic inland basement marked by a prominent anomaly maximum cra35 [72.70°S, 155.67°E] (Ferraccioli et al., 2017). However, the alternate age of ca. 250 Ma also has been inferred for the sedimentary basins based on the Permian-to-Triassic sedimentary rocks intruded by the Ferrar tholeiites that crop out along the western Horn Bluff edge and the eastern edge of the Cook Ice Shelf at Mount Obruchev (MO; Mawson, 1940; Pavlov, 1958; Ravich et al., 1968).

The WSB's deep western basins, which provide strong topographic control on the Ninnis Glacier (NG), are marked by anomaly minima cra36 [68.74°S, 146.43°E]. These minima possibly map the Paleoproterozoic crustal boundary between an inferred Archean crustal ribbon or steep-sided shallow trough cra37 [67.08°S, 141.2°E] and the partially exposed Paleoproterozoic rift basins along the coast next to the Terre Adélie Craton (Ferraccioli et al., 2009).

The new survey data in Wilkes Land map a prominent 2,100 km-long elongate magnetic low with elements cra38 [68.51°S, 145.25°E], cra39 [74.76°S, 143.84°E], cra40 [78.56, 144.29°E], and cra41 [83.93°S, 146.82°E] that marks the Archean-to-Mesoproterozoic edge of the Mawson continent consisting of Australia's Gawler Craton (Payne et al., 2009) and East Antarctica's Terre Adélie Craton (Gapais et al., 2008). This N/S-trending magnetic lineament may image the Mertz Shear Zone from the South Pole toward the George V Coast. The shear zone underlies the Mertz Glacier (MzG) and may mark a lithospheric suture related to the collisional and transpressional Paleoproterozoic tectonics (Ferraccioli et al., 2017). In addition, the N/S-trending system of anomaly minima along roughly 145°E potentially indicates the effects of major rift-basins beneath the WSB, where Ross-age terranes in Victoria Land and the TAM may transition into East Antarctica's Precambrian interior.

For the George V Coast, the roughly 100–300 km-diameter magnetic maxima cra42 [67.79°S, 147.24°E] and cra43 [71.62°S, 154.32°E] (Damaske et al., 2003; Ferraccioli et al., 2003) involve only sparse outcrop constraints of early Paleozoic plutons (Finn et al., 2006). Although these near-surface anomalies have been interpreted for the effects of igneous Precambrian or Jurassic rocks (Damaske et al., 2003; Talarico et al., 2001), they may also signal the presence of Paleozoic sources because they are similar to the magnetic signatures of the Australian and Antarctic Paleozoic plutons (Ferraccioli et al., 2002; Finn et al., 1999). Comparable wavelength and amplitude magnetic maxima also have been inferred for the effects of early Paleozoic plutons in the TAM of southern Victoria Land (Bozzo et al., 1997; Ferraccioli & Bozzo, 1999; Ferraccioli et al., 2003). However, the magnetic

signatures of Paleozoic plutons are inconsistent across the TAM, where many granites exhibit marginally positive relative magnetizations (Damaske & Bosum, 1993; Ferraccioli et al., 2002) or even relatively negative magnetizations as found in the central TAM (Goodge et al., 2004). These anomalies are strongly suppressed at altitudes of 75 km and higher in Figure 8, and thus are poorly imaged by the Swarm mission data.

The white ellipses of Figure 4 include 56 strongly negative near-surface magnetic anomalies with amplitudes down to $-2,650$ nT. A few of these anomalies have been described in detail, including the one cra44 [71.34°S, 13.48°E] in central DML (Choi, 2005) and another cra45 [76.11°S, 130.2°E] over the WSB (Studinger et al., 2004). The first case was attributed to the effects of ca. 620 Ma Wohltat massif anorthosites, even though specimens with the corresponding magnetic remanence have not been observed (Paech & Marcinkowski, 2005). No source speculations are available for the second case of the strongly negative anomaly over the WSB. The intense minima fade quickly with altitude in Figure 8 and appear to be irresolvable at Swarm altitudes.

In northern Victoria Land, the intense short-wavelength anomaly minima (e.g., cra46 [73.14°S, 165.53°E], cra47 [72.69°S, 167.33°E], and cra48 [71.31°S, 170.20°E]) have been mostly attributed to the Late Cenozoic McMurdo volcanics or Meander intrusives that crop out over the Adare, Daniel, and Hallett peninsulas and in the Victory Mountains (LeMasurier, 1990; Tonarini et al., 1997). Although no outcrop observations of strong reversely magnetized rocks are available, the highly near-circular aeromagnetic anomalies commonly mark large alkaline intrusions (Armadillo et al., 2007; Bosum et al., 1989). These high-frequency minima also fade quickly with altitude in Figure 8 so that they are not resolved at Swarm altitudes.

South of Law Dome cra49 [66.73°S, 112.83°E] in Wilkes Land, eight intensely negative anomalies form a continuous belt that is roughly 650 km in length. Aitken et al. (2014) grossly linked several of these minima with weakly magnetic intrusions of Australia's Albany-Fraser Province and their 'West Mawson Craton.' The anomalies cra50 [67.06°S, 112.66°E], cra51 [66.60°S, 112.23°E], and cra52 [66.49°S, 113.56°E] over Law Dome may represent widely spaced components of a single anomaly cra53 [66.69°S, 112.76°E] covering an area of about 9,500 km². Accordingly, this anomaly may map out another giant mafic/ultramafic intrusive complex of the Earth like Norway's Bjerkreim-Sokndal layered intrusion (McEnroe et al., 2001), the Coompana Block gabbro in Australia (Dutch et al., 2017), and the granitic-gneiss complex in the Adirondack Mountains of North America (McEnroe & Brown, 2000). The anomalies persist in Figure 8 up to about 100 km altitude, but quickly fade out at higher altitudes, and thus are poorly resolved by the Swarm anomalies.

Insights on the possible sources of Wilkes Land's intense anomaly minima may result from studying comparable anomalies of the conjugate Australian plate like the intense minima that characterize, for example, the Albany-Fraser Orogen, Officer Basin, and Coompana Block (Milligan et al., 2010). A belt of some eight to 10 of these magnetic minima arcs along the western and southern Australian coast through the Officer Basin to the Musgrave Province to suggest a common underlying crustal origin for the anomalies. Boreholes targeting circular anomalies in the Coompana Block intersected mafic-ultramafic gabbro and dolerite intrusions at the approximate depth of 300 m (Foss et al., 2016). However, for the Albany-Fraser Orogen, compositionally similar bodies may form part of the same intrusive suite, but at considerably greater depths of about 8–19 km.

The relative ages and contact relationships of the SW Australian intrusive bodies are constrained by the Coompana Magnetic Anomaly (CMA), which was modeled as a multi-phase intrusive complex involving an initial deep crustal disk-like intrusion that subsequently developed pipe-like feeder intrusions in the upper crust (Wise et al., 2016). The intrusive complex's interpreted age is between ca. 1,120 Ma and 860 Ma. Furthermore, a Bouguer gravity anomaly minimum is coincident with the CMA minimum to suggest that the source body's density is somewhat less than that of the mafic-to-ultramafic or highly altered crust (Foss et al., 2016). These correlations, accordingly, may reflect the effects of a gigantic collapsed caldera or diatreme, or a Sudbury-like impact basin with post-impact magmatic intrusions in the basin's outer ring (Zengerer, 2017). Alternative interpretations suggest that they may mark a crustal basin, an anorthosite complex, or some other low-density crustal feature carrying reversed remanent magnetization (Foss et al., 2018).

The intensely negative anomalies in southern Australia and Wilkes Land clearly involve enigmatic origins. However, the regional Coompana Province drilling program's results (Dutch et al., 2017) can help to reduce uncertainties of the anomaly inversions for their possible crustal magnetization attributes. The drilling program revealed a predominantly igneous history that possibly extends into the Neoproterozoic. The cored lithologies include deformed and migmatitic low magnetization and density orthogneisses, undeformed porphyritic granites

from a NE-trending band of highly magnetic plutons, and undeformed gabbro-norites from remanently magnetized, high-density late-stage intrusions. The CDP005 drillhole at the site of the strong reversely magnetized CMA intersected massive megacrystic granite, suggesting that the source of the large, reversely polarized CMA lies deeper than the basement's surface (Dutch et al., 2017).

3.3. Southern Ocean Magnetic Anomalies

Figures 4 and 6 readily illustrate the magnetic anomaly contrast between continental and oceanic crust. Specifically, relatively complex magnetic anomaly patterns characterize the older and thicker recycled continental crust, whereas fairly uniform seafloor spreading anomaly patterns mark the newer and thinner oceanic crust. In the northern Weddell Sea, the pattern of NE/SW-striking seafloor spreading anomalies reflects mid-ocean ridge effects that accommodated the late Jurassic and Cretaceous motions of South America and Antarctica (Kovacs et al., 2002). In the central part of the Weddell Sea up through Swarm altitudes, linear magnetic anomaly maxima correspond to earlier phases (initial stages) of rifting between the South American and Antarctic plates. The northern Weddell Sea displays a linear minimum associated with later stages of rifting.

The aeromagnetic data from the Riiser-Larsen and eastern Weddell Seas tightly constrain the breakup of Gondwana (Jokat et al., 2003; König & Jokat, 2006). Oceanic crust started to form in the Riiser-Larsen Sea and conjugate Mozambique Basin at ca. 159 Ma. Further west, between ca. 146 and 143 Ma, break up was initiated by the development of a mid-ocean ridge that propagated eastwards through the eastern Weddell Sea at about 63 km/Myr (Jokat et al., 2003; Leinweber & Jokat, 2012).

The more than 430,000 line-km of new airborne and marine magnetic survey data that were processed into the ADMAP-2 near-surface anomaly grid of Figure 4 greatly facilitate geologic investigations of East Antarctica's margin (e.g., Golynsky et al., 2013; Leinweber & Jokat, 2012). The new data help illuminate, for example, the tectonic and magmatic processes during the breakup of Africa, India, Australia and East Antarctica, and also highlight coverage gaps for the planning of future surveys. Over the Maud Rise and Kerguelen Plateau up through Swarm altitudes, pronounced magnetic anomaly maxima mark the possible effects of the extensive vulcanism from the related mantle hot spots.

The prominent curvilinear Antarctic Continental Margin Magnetic Anomaly (ACMMA) in Figures 4 and 6 skirts the coastlines of DML and Enderby Land and continues as far as the MzG in Adélie Land (Golynsky, Alyavdin, et al., 2002). The anomaly appears to represent continental breakup processes for perhaps the longest continuous tectonomagmatic feature in Antarctica. In the Cooperation Sea, the pronounced off-shore Enderby Basin Anomaly (EBA) extends roughly 1,680 km from the Kerguelen Plateau to the Cosmonaut Sea (Golynsky et al., 2007). The strong positive anomaly marks a basement rise with commensurate enhancements of crustal thickness and seismic velocity about 300 km seaward of East Antarctica's continental shelf (Stagg et al., 2005). The anomaly has been variously interpreted for the effects of a continent-ocean boundary, the continental remnants or scar of a propagating mid-ocean ridge, and the change in magma supply to a mid-ocean ridge (Davis et al., 2019; Gaina et al., 2007). Major elements of the ACMMA that are apparent in the Swarm observations include the Weddell Sea-to-Riiser Larsen Sea, the Cosmonaut Sea-and-western Cooperation Sea, and the Cooperation Sea-to-Mawson Sea segments. These segments accordingly may mark voluminous intrusions of the East Antarctic crustal margin during initial stages of Gondwana rifting. By Figure 8, however, the EBA is discernible only up to about 75 km altitude, and thus is poorly mapped by Swarm's observations.

Magnetic anomalies of the Southern Ocean around East Antarctica significantly constrain the tectonic evolution of the seafloor (Golynsky et al., 2013). In particular, strong near-surface and satellite magnetic anomaly maxima overlie the southern margin of the Kerguelen Plateau, as well as the Maud Rise and neighboring Astrid Ridge. These maxima may reflect the effects of the basaltic veneers overlying stretched continental crustal fragments that are either separated from the Antarctic's continental margin (e.g., southern Kerguelen Plateau) or connected to it (e.g., Astrid Ridge). The anomaly maxima also mark thickened igneous crust formed within the oceanic basins (e.g., Maud Rise).

Prominent Swarm magnetic anomalies along the East Antarctic margin include the NE/SW-trending anomaly minimum cra54 [65.23°S, 23.43°E] over the Riiser Larsen Sea that possibly marks relatively thinned oceanic crust hosting thickened sedimentary deposits or another crustal demagnetizing effect (Figures 7a and 8). Further east, the western flank cra55 [64.20°S, 40.65°E] of the regional maximum in the Cosmonaut Sea overlies seafloor

spreading that developed during the stable Cretaceous Normal Superchron over the ca. 90–118 Ma period (Jokat et al., 2010). The enhanced magnetization effects of Kerguelen volcanism apparently are reflected by the elongate maximum with elements cra56 [60.99°S, 71.70°E] and cra57 [61.92°S, 90.51°E] over the off-shore coastal Enderby Basin and the Davis Sea, respectively.

The magnetic data of the Enderby Basin (EBA) and the Shackleton Basin (SB) map at least 300 km of deposits from the Early Cretaceous Kerguelen Volcanic Province (Golynsky et al., 2013). Initiated in ca. 120–110 Ma (Frey et al., 2000), the massive hot spot volcanism emplaced volcanoclastic material and lava flows onto both oceanic and continental crust. The magnetic effects of these volcanic rocks complicate interpreting the seafloor spreading anomalies and recognizing, for example, the central Enderby Basin's inactive spreading center (Golynsky et al., 2013; Stagg et al., 2005). Similar basaltic flows occur near the Astrid Rise in the Riiser-Larsen Sea (Leitchenkov et al., 2008), but their masking effects are less significant for clarifying the basin's seafloor spreading anomalies M0-M24.

Off-shore of the Adélie Rift Block (ARB), the seafloor spreading history is poorly resolved (Colwell et al., 2006; Golynsky et al., 2013) and regional satellite and near-surface magnetic minima cover the Dumont d'Urville Sea into the Mawson Sea. The near-surface magnetic anomalies in combination with the continental lithologies dredged from the anomalously shallow bathymetry (Yuasa et al., 1997), and the complementary atypical free-air gravity anomaly minimum point to possibly hyperextended underlying Australian continental crust. Furthermore, the Spencer Fracture zone at the ARB's eastern edge may constitute the sheared margin of Gondwana that was conjugate to Australia's margin west of Tasmania.

The least-surveyed segment of the Southern Ocean lies off West Antarctica's Pacific margin. The Amundsen and eastern Ross Seas are particularly poorly sampled, even with the inclusion of the roughly 83,000 line-km of magnetic survey data collected during 1992–2007 (e.g., Cande et al., 1995). These data refine the early history of the diverging Bellingshausen and Pacific plates including the New Zealand–West Antarctica rifting, and the pre-spreading locations of the Campbell Plateau relative to the margins of Marie Byrd Land and the Ross Sea Embayment and their offshore pendants at Iselin Bank (Cande et al., 2000; Eagles et al., 2004; Wobbe et al., 2012).

The Swarm magnetic anomaly observations of Figure 5, by contrast, generally characterize the Bellingshausen Sea, Amundsen Sea, and the western Ross Sea sectors of the Pacific Ocean with broad relative minima. However, the strongly positive PMA in the near-surface grid is marked by prominent Swarm maxima along the West Antarctic Peninsula and Marie Byrd Land coastlines. The maxima extend further northwestwards across the Ross Sea to intersect the broad E/W-trending maximum with the eastern flank covering the Pacific–Antarctic Ridge system's younger elements (Müller et al., 2008). For the most part, oceanic crust with enhanced heat flow tends to exhibit both near-surface and satellite magnetic anomaly maxima.

In the off-shore Adare Basin (AB) of the northern Ross Sea, N/NW-trending aeromagnetic anomalies infer Cenozoic seafloor spreading in the oceanic extension of the WARS from West Antarctica (Cande & Stock, 2006). Further details mapped by the high-quality aeromagnetic surveying include the transition between the WARS and the off-shore AB involving several Eocene–Oligocene rotations that constrain the relative crustal motions of East and West Antarctica (Damaske et al., 2007; Granot et al., 2013). The results infer the transition of seafloor spreading in the AB along WARS-strike to continental extension within the off-shore Victoria Land Basin that progressed further inland as a transcurrent plate margin (Davey et al., 2016; Granot et al., 2013). In the Swarm data, the WARS' NE extension across the Ross Sea is marked by a prominent regional maximum that lies along the western boundary of the regional minimum over the Ross Ice Shelf and western Sea, TAM, and Victoria Land.

Off the Antarctic Peninsula's Pacific margin, downward continued anomalies from the ICEGRAV (Forsberg et al., 2018), USAC (LaBrecque et al., 1986), and Project Magnet (Hittleman et al., 1996) aeromagnetic surveys significantly enhanced details of the seafloor spreading and fracture zone anomalies for further insights on the tectonic interactions of the Phoenix and West Antarctic plates (Eagles, 2004). However, these anomaly features appear to fade out quickly with altitude and thus are poorly resolved in the Swarm observations.

Over the broad continental shelf in the ASE, helicopter and shipborne magnetic surveys in 2006 and 2010 filled in the biggest coverage gap in the ADMAP-1 compilation and obtained significant new insights on the region's crustal structure and tectonic history (Gohl et al., 2013). These magnetic anomalies constrain the tectonic and magmatic products of long-lived crustal extension that multiple failed rifts accommodated. The magnetic data

clearly image a hinge zone cra58 [74.18°S, 117.65°W], where the basement rocks crop out south of it, and dive north of it beneath thick sedimentary cover.

The strongly positive near-surface PMA (Figure 4) complements the prominent Swarm maximum along the West Antarctic peninsula and Marie Byrd Land coastlines (Figure 8). The PMA appears to mark crustal fragments of West Antarctica's margin from the initial Cretaceous separation of New Zealand and West Antarctica.

4. Conclusions

The ADMAP-2s compilation (Figures 6 and 8) is the most wide-ranging and self-consistent presentation to date of the Antarctic's crustal magnetic anomalies as surveyed since the IGY' 1957–1958 by numerous international magnetic campaigns with disparate mapping parameters. The ADMAP-2s anomaly predictions are based on a spherical coordinate distribution of crustal magnetic point dipoles with magnetic volume susceptibilities least squares estimated from the joint inversion of the gap-filled ADMAP-2 anomalies at the Earth's mean geocentric radius of 6,371.2 km (Figure 6) and the satellite anomaly estimates from the Swarm mission at 250 km above the Earth's mean geocentric radius (Figure 5). Its magnetic anomalies from the near-surface to satellite altitudes reflect a detailed tapestry of crustal terranes defined by diverse lithologies, ages, thermal states, and metamorphic grades (e.g., Ferraccioli et al., 2011; Golynsky, 2007; McLean et al., 2009; Mieth & Jokat, 2014).

Offshore, for example, the ADMAP-2s model accommodates the 430,000 line-km of new airborne and ship survey data from the ADMAP-2 compilation that illuminate Antarctica's continent-ocean transition zones and significantly transform our view of the East Antarctic continental margins. The prominent near-surface Antarctic continental margin magnetic anomaly (ACMMA) may mark voluminous intrusions of the crustal margin during the initial stages of Gondwana rifting. However, its segments that extend from the Weddell Sea to Riiser Larsen Sea, the Cosmonaut Sea to the western Cooperation Sea, and the Cooperation Sea to the Mawson Sea involve magnetic effects which are also apparent in the Swarm observations. Additionally, Swarm magnetic anomaly maxima readily mark the ridges, plateaus, and other enhanced geothermal heat flow features of the oceanic crust. However, these maxima are effectively masked in the near-surface anomaly grid by the strong high-frequency effects of the marine crust that, in turn, are poorly mapped at satellite altitudes.

Inland, the ADMAP-2s compilation provides important new constraints on the enigmatic geology of the Gamburtsev Subglacial Mountains, Prince Charles Mountains, Wilkes Land, Dronning Maud Land, and other poorly explored Antarctic areas. It offers new insights on the Antarctic's crustal properties and effects of global tectonic processes. It also links widely separated outcrops to help unify disparate geologic and geophysical studies. For example, in PEL, aeromagnetic surveying imaged the Stenian-aged accretional orogen of a length that exceeds 1,000 km. However, the disrupted crustal effects from the collision of the Indian and Asian tectonic plates may obscure the effects of its possible extension into neighboring Gondwanan India. On the other hand, marking the Mawson Craton's southern boundary along 85.5°S between 157°E and 135°E is consistent with well-defined magnetic anomaly maxima in both the near-surface and Swarm observations. Thus, the rocks exposed in the Shackleton Ranges may not be part of the Mawson Craton (Boger, 2011), even though they formed in the Late Paleoproterozoic orogenesis with Terre Adélie Land (Will et al., 2009). Also, within the East African-Antarctic Orogen, a major tectonic block's edge and/or a suture zone have/has been inferred from the near-surface FMA. However, the ADMAP-2s data suggest the Forster Magnetic Anomaly (FMA) is severely suppressed at higher altitudes so that its interpretation for the effects of a pervasive magnetization feature of the crust is suspect.

In general, the ADMAP-2s data characterize the diverse magnetic effects of Proterozoic-Archean cratons, Proterozoic-Paleozoic mobile belts, Paleozoic-Cenozoic magmatic arc systems and the rift basins between East and West Antarctica (e.g., Aitken et al., 2014; Ferraccioli et al., 2011; Gohl et al., 2013; Jokat et al., 2010; Jordan et al., 2013). They also help resolve basement terranes and the intervening suture zones, intra-continental and continental margin rift basins, and regional plutonic and volcanic features like the Ferrar dolerites and Kirkpatrick basalts (e.g., Aitken et al., 2016; Ferraccioli & Bozzo, 2003; Ferraccioli et al., 2005, 2011; Golynsky, Golynsky, et al., 2006; Goodge & Finn, 2010; Mieth et al., 2014). In combination with gravity, ice-probing radar, and other geophysical and geological data, the ADMAP-2s model facilitates studying continental rifting, intraplate orogenesis and basin subsidence, subduction and terrane accretion, seafloor spreading, and other large-scale geological processes of the Antarctic.

Satellite magnetometer observations of crustal magnetic anomalies also provide important constraints for augmenting the ADMAP-2 compilation's regional near-surface data coverage gaps that are especially severe for areas offshore of West Antarctica and in East Antarctica. For this study, the fill values were estimated from the joint inversion of the local near-surface and Swarm satellite magnetic anomaly data (Kim et al., 2004, 2007). However, despite applying significant near-surface and satellite magnetic anomaly boundary conditions, the fill estimates must be used with care because they are not unique and subject to data and processing errors.

Combining Swarm satellite magnetic observations with the near-surface ADMAP-2 grid via the spherical coordinate point dipole model yields further insights on the crustal anomaly components in both datasets. By honoring the data sets in the least-squares sense, the spherical point dipole model improves the crustal magnetic anomaly predictions at the intervening altitudes where conventional downward or upward continuation of each input data set is unreliable. Regionally pervasive magnetization enhancements of the crust typically are marked by near-surface magnetic anomalies that persist up through Swarm altitudes, whereas relatively superficial magnetization enhancements tend to involve anomalies that fade quickly with increasing altitude.

Prominent near-surface and satellite magnetic anomaly maxima along the continental margins, for example, appear to mark the effects of rift-related magmatic products. The largest amplitude anomaly maximum in the Swarm data is over northern Wilkes Land, however, where giant meteorite impact in a normal-polarity geomagnetic field at ca. 260 Ma may have further amplified crustal magnetization. This enhanced magnetic crust also appears to extend into southcentral Australia to produce a prominent conjugate satellite magnetic anomaly maximum (von Frese et al., 1986, 2013).

Satellite and near-surface magnetometers obtain limited accuracy measurements that strongly emphasize the respective lower and higher frequency attributes of the anomalies. Thus, standard downward and upward continuations of the respective magnetometer data are largely ineffective in reconciling the anomalies over large altitude variations (e.g., Kim & von Frese, 2017; Kim et al., 2013). In general, multiple altitude anomaly measurements offer substantial interpretational advantages over single altitude observations.

The ADMAP-2 and -2s grids of scalar total magnetic field anomaly values at the interval of 1.5 km may be freely downloaded from the ADMAP website maintained by the Korea Polar Research Institute (<http://admap.kopri.re.kr>). The website also provides complete access to the survey data as supplied and reprocessed for the ADMAP-2 compilation, as well as ADMAP's reports to SCAR on its activities and the status of magnetic surveying in the Antarctic. It also provides the point dipole magnetic susceptibilities for estimating the Antarctic's magnetic anomaly potential, vector, and tensor components at any spherical coordinate on or above the Earth's mean geocentric radius.

ADMAP's activities demonstrate the power of international collaboration in producing and updating a coherent digital magnetic anomaly database and map of the Antarctic. The synthesis of the individual magnetic surveys into the ADMAP compilation greatly enhances their utility for geological studies of the Antarctic region south of 60°S.

Data Availability Statement

Swarm anomalies were obtained from the spherical harmonic model, LCS-1, downloaded from <http://www.spacecenter.dk/files/magnetic-models/LCS-1/>. This study's anomaly grids can be generated by the ADMAP-2s equivalent magnetic point source model available from http://admap.kopri.re.kr/admapdata/ADMAP_2S_EPS_20km.zip with MATLAB® driver codes available from http://admap.kopri.re.kr/admapdata/JGR2022_Kim_etal.zip and its mirrored site at <https://admap.kongju.ac.kr>.

References

- Aitken, A. R. A., Betts, P. G., Young, D. A., Blankenship, D. D., Roberts, J. L., & Siegert, M. J. (2016). The Australo-Antarctic Columbia to Gondwana transition. *Gondwana Research*, 29(1), 136–152. <https://doi.org/10.1016/j.gr.2014.10.019>
- Aitken, A. R. A., Young, D., Ferraccioli, F., Betts, P. G., Greenbaum, J. S., Richter, T. G., et al. (2014). The subglacial geology of Wilkes land, East Antarctica. *Geophysical Research Letters*, 41(7), 2390–2400. <https://doi.org/10.1002/2014gl059405>
- Armadillo, E., Ferraccioli, F., Zunino, A., Bozzo, E., Rocchi, S., & Armienti, P. (2007). Aeromagnetic search for Cenozoic magmatism over the Admiralty mountains block (East Antarctica). In A. K. Cooper, et al. (Eds.), *Presented at the Antarctica: A keystone in a changing world—online proceedings of the 10th ISAES* (Vol. 1047). USGS Open-File Report.

Acknowledgments

We thank the members of SCAR's ADMAP expert group and their affiliated institutions for contributing raw and processed magnetic survey data and cooperating in developing the ADMAP-2 compilation. We also thank J. Galindo-Zaldívar and two anonymous reviewers for their constructive comments. Elements of this research were supported by the research grant of Kongju National University in 2021 and the Republic of Korea's National Research Foundation grant (NRF2019R-1F1A1051876) to HRK funded by the Korean Ministry of Science. SCAR supported the activities of the ADMAP expert group, and grants PM15040 and PE17050 from the Korea Polar Research Institute (KOPRI) partially funded aspects of this study at the All-Russian Scientific Research Institute for Geology and Mineral Resources of the World Ocean (VNIIOkeangeologia). Swarm anomalies were obtained from the spherical harmonic model, LCS-1, downloaded from <http://www.spacecenter.dk/files/magnetic-models/LCS-1/>. This study's anomaly grids can be generated by the ADMAP-2s equivalent magnetic point source model available from http://admap.kopri.re.kr/admapdata/ADMAP_2S_EPS_20km.zip with MATLAB® driver codes available from http://admap.kopri.re.kr/admapdata/JGR2022_Kim_etal.zip and its mirrored site at <https://admap.kongju.ac.kr>.

- Asgharzadeh, M. F., von Frese, R. R. B., & Kim, H. R. (2008). Spherical prism magnetic effects by Gauss-Legendre quadrature integration. *Geophysical Journal International*, 173(1), 315–333. <https://doi.org/10.1111/j.1365-246x.2007.03692.x>
- Behrendt, J. C. (1964). Distribution of narrow-width magnetic anomalies in Antarctica. *Science*, 144(3621), 993–995. <https://doi.org/10.1126/science.144.3621.993>
- Behrendt, J. C. (1999). Crustal and lithospheric structure of the West Antarctic Rift System from geophysical investigations—A review. *Global and Planetary Change*, 23(1–4), 25–44. [https://doi.org/10.1016/s0921-8181\(99\)00049-1](https://doi.org/10.1016/s0921-8181(99)00049-1)
- Behrendt, J. C., Saltus, R., Damaske, D., McCafferty, A., Finn, C. A., Blankenship, D., & Bell, R. E. (1996). Patterns of late Cenozoic volcanic and tectonic activity in the West Antarctic rift system revealed by aeromagnetic surveys. *Tectonics*, 15(3), 660–676. <https://doi.org/10.1029/95tc03500>
- Bingham, R. G., Ferraccioli, F., King, E. C., Larter, R. D., Pritchard, H. D., Smith, A. M., & Vaughan, D. G. (2012). Inland thinning of West Antarctic ice sheet steered along subglacial rifts. *Nature*, 487(7408), 468–471. <https://doi.org/10.1038/nature11292>
- Blankenship, D. D., Bell, R. E., Hodge, S. M., Brozena, J. M., Behrendt, J. C., & Finn, C. A. (1993). Active volcanism beneath the West Antarctic ice sheet and implications for ice-sheet stability. *Nature*, 361(6412), 526–529. <https://doi.org/10.1038/361526a0>
- Blankenship, D. D., Young, D. A., Richter, T. G., & Greenbaum, J. S. (2011). IceBridge BGM-3 Gravimeter L2 Geolocated Free Air Anomalies, version 1. NASA Distributed Active Archive Center (DAAC) at the National Snow and Ice Data Center (NSIDC). *Doi*, 10.
- Boger, S., & Wilson, C. (2003). Brittle faulting in the Prince Charles Mountains, East Antarctica: Cretaceous-transensional tectonics related to the break-up of Gondwana. *Tectonophysics*, 367(3–4), 173–186. [https://doi.org/10.1016/s0040-1951\(03\)00125-2](https://doi.org/10.1016/s0040-1951(03)00125-2)
- Boger, S. D. (2011). Antarctica – Before and after Gondwana. *Gondwana Research*, 19, 335–371. <https://doi.org/10.1016/j.gr.2010.09.003>
- Bosum, W., Damaske, D., Roland, N., Behrendt, J., & Saltus, R. (1989). The GANOVEX IV Victoria Land/Ross Sea aeromagnetic survey: Interpretation of anomalies. *Geologisches Jahrbuch E*, 38, 153–230.
- Bozzo, E., Caneva, G., Chiappini, M., Colla, A., Damaske, D., Ferraccioli, F., et al. (1997). Total magnetic anomaly map of Victoria Land (central-southern part), Antarctica. *The Antarctic region: Geological evolution and processes*. Terra Antarctica Publication, 1165–1.
- Burton-Johnson, A., & Riley, T. (2015). Autochthonous v. accreted terrane development of continental margins: A revised in situ tectonic history of the Antarctic Peninsula. *Journal of the Geological Society*, 172(6), 822–835. <https://doi.org/10.1144/jgs2014-110>
- Cande, S. C., Raymond, C. A., Stock, J., & Haxby, W. F. (1995). Geophysics of the Pitman fracture zone and Pacific-Antarctic Plate motions during the Cenozoic. *Science*, 270(5238), 947–953. <https://doi.org/10.1126/science.270.5238.947>
- Cande, S. C., & Stock, J. M. (2006). Constraints on the timing of extension in the Northern basin, Ross Sea. In D. K. Futterer, D. Damaske, G. Gleinschmidt, H. Miller, & F. Tessensohn (Eds.), *Antarctica: Contributions to global earth sciences*. Springer-Verlag.
- Cande, S. C., Stock, J. M., Müller, R. D., & Ishihara, T. (2000). Cenozoic motion between east and west Antarctica. *Nature*, 404(6774), 145–150. <https://doi.org/10.1038/35004501>
- Chiappini, M., von Frese, R. R., & Ferris, J. (1998). Effort to develop magnetic anomaly database aids Antarctic research. *Eos, Transactions American Geophysical Union*, 79(25), 290. <https://doi.org/10.1029/98eo00214>
- Chiappini, M., & von Frese, R. R. B. (1999). Advances in Antarctic geomagnetism—Preface. *Annali di Geofisica*, 42.
- Choi, S. (2005). 3-D Aeromagnetic modelling in the Grubergerbirge Area, Central Dronning Maud Land, East Antarctica. *Geologisches Jahrbuch - Reihe B*, 97, 101.
- Colwell, J. B., Stagg, H. M., Direen, N. G., Bernardel, G., & Borissova, I. (2006). The structure of the continental margin off Wilkes Land and Terre Adelie coast, east Antarctica. In D. K. Futterer, D. Damaske, G. Gleinschmidt, H. Miller, & F. Tessensohn (Eds.), *Antarctica: Contributions to global earth sciences* (pp. 327–340). Springer-Verlag.
- Daczko, N. R., Halpin, J. A., Fitzsimons, I. C., & Whittaker, J. M. (2018). A cryptic Gondwana-forming orogen located in Antarctica. *Scientific Reports*, 8(1), 1–9. <https://doi.org/10.1038/s41598-018-26530-1>
- Damaske, D. (1999). Merging aeromagnetic data collected at different levels: The GEOMAUD survey. *Annali di Geofisica*, 42(2), 153–159. <https://doi.org/10.4401/ag-3710>
- Damaske, D., Behrendt, J., McCafferty, A., Saltus, R., & Meyer, U. (1994). Transfer faults in the western Ross Sea: New evidence from the McMurdo Sound/Ross ice shelf aeromagnetic survey (GANOVEX VI). *Antarctic Science*, 6(3), 359–364. <https://doi.org/10.1017/s0954102094000556>
- Damaske, D., & Bosum, W. (1993). Interpretation of the aeromagnetic anomalies above the lower Rennick glacier and the adjacent polar plateau west of the USARP Mountains. *Geologisches Jahrbuch. Reihe E, Geophysik*, 1993(47), 139–152.
- Damaske, D., Ferraccioli, F., & Bozzo, E. (2003). Aeromagnetic anomaly investigations along the Antarctic coast between Yule Bay and Mertz Glacier. In D. Damaske, & E. Bozzo (Eds.), *Scientific results from the joint German-Italian 1999–2000 Antarctic expedition* (Vol. 10, pp. 85–96). Terra Antarctica.
- Damaske, D., & Finn, C. (1996). Explanatory notes on the 1: 250,000 maps of the anomalies of the total magnetic field, Bowers Mountains, Antarctica. *Aeromagnetic Survey during the Expedition GANOVEX VI*, 91(1), map. 10.
- Damaske, D., Läufer, A., Goldmann, F., Möller, H., & Lisker, F. (2007). Magnetic anomalies north-east of Cape Adare, northern Victoria Land (Antarctica), and their relation to onshore structures. In A. K. Cooper, & C. R. Raymond (Eds.), *Antarctica: A keystone in a changing world*. The National Academies Press. <https://doi.org/10.3133/ofr20071047srp016>
- Davey, F., Granot, R., Cande, S., Stock, J., Selvans, M., & Ferraccioli, F. (2016). Synchronous oceanic spreading and continental rifting in West Antarctica. *Geophysical Research Letters*, 43(12), 6162–6169. <https://doi.org/10.1002/2016gl069087>
- Davis, J. K., Lawver, L. A., Norton, I. O., Dalziel, I. W., & Gahagan, L. M. (2019). The crustal structure of the Enderby Basin, East Antarctica. *Marine Geophysical Researches*, 40(1), 1–16. <https://doi.org/10.1007/s11001-018-9356-5>
- Dutch, R. A., Pawley, M., Tylkowski, L., Wise, T., Heath, P., Lockheed, A., et al. (2017). *PACE Copper Coompana drilling Project: Drillhole CDP008 preliminary field-data report*. Department of the Premier and Cabinet.
- Eagles, G. (2004). Tectonic evolution of the Antarctic–Phoenix plate system since 15 Ma. *Earth and Planetary Science Letters*, 217(1–2), 97–109. [https://doi.org/10.1016/s0012-821x\(03\)00584-3](https://doi.org/10.1016/s0012-821x(03)00584-3)
- Eagles, G., Gohl, K., & Larter, R. D. (2004). Life of the Bellingshausen plate. *Geophysical Research Letters*, 31(7), L07603. <https://doi.org/10.1029/2003gl019127>
- Fanning, C. M., Daly, S. J., Bennett, V. C., Ménot, R. P., Peucat, J. J., Oliver, R. L., & Monnier, O. (1995). The “Mawson block”: Once contiguous Archean to Proterozoic crust in the East Antarctic shield and Gawler craton, Australia. In *VII International Symposium on Antarctic Earth Sciences* (Spec. Vol.). Terra Antarctica.
- Ferraccioli, F., Armadillo, E., Young, D., Blankenship, D., Jordan, T., & Siegert, M. (2017). Geological controls on bedrock topography and ice sheet dynamics in the Wilkes Subglacial Basin sector of East Antarctica. In *Presented at the EGU general assembly conference abstracts* (p. 18157).

- Ferraccioli, F., Armadillo, E., Zunino, A., Bozzo, E., Rocchi, S., & Armentieri, P. (2009). Magmatic and tectonic patterns over the Northern Victoria Land sector of the Transantarctic Mountains from new aeromagnetic imaging. *Tectonophysics*, 478(1–2), 43–61. <https://doi.org/10.1016/j.tecto.2008.11.028>
- Ferraccioli, F., & Bozzo, E. (1999). Inherited crustal features and tectonic blocks of the Transantarctic Mountains: An aeromagnetic perspective (Victoria Land, Antarctica). *Journal of Geophysical Research*, 104(B11), 25297–25319. <https://doi.org/10.1029/1998jb900041>
- Ferraccioli, F., & Bozzo, E. (2003). Cenozoic strike-slip faulting from the eastern margin of the Wilkes Subglacial Basin to the western margin of the Ross Sea rift: An aeromagnetic connection. *Geological Society, London, Special Publications*, 210(1), 109–133. <https://doi.org/10.1144/gsl.sp.2003.210.01.07>
- Ferraccioli, F., Bozzo, E., & Capponi, G. (2002). Aeromagnetic and gravity anomaly constraints for an early Paleozoic subduction system of Victoria Land, Antarctica. *Geophysical Research Letters*, 29(10), 44–1–44–4. <https://doi.org/10.1029/2001gl014138>
- Ferraccioli, F., Damaske, D., Bozzo, E., Spano, M., & Chiappini, M. (2000). Magnetic anomaly patterns over crustal blocks of the King Edward VII Peninsula, Marie Byrd Land, West Antarctica. *Annali di Geofisica*, 43(2), 229–241.
- Ferraccioli, F., Damaske, D., Bozzo, E., & Talarico, F. (2003). The Matushevich aeromagnetic anomaly over Oates Land, East Antarctica. *Terra Antarctica*, 10, 221–228.
- Ferraccioli, F., Finn, C. A., Jordan, T. A., Bell, R. E., Anderson, L. M., & Damaske, D. (2011). East Antarctic rifting triggers uplift of the Gamburtsev mountains. *Nature*, 479(7373), 388–392. <https://doi.org/10.1038/nature10566>
- Ferraccioli, F., Forsberg, R., Eagles, G., Jacobs, J., Martos, Y., Jordan, T. A., et al. (2016). Investigating East Antarctic basement provinces from the Shackleton range to Dronning Maud Land with new magnetic and gravity compilations. In *Presented at the 35th international geological congress, Cape Town, South Africa*. Retrieved from <https://www.americangeosciences.org/igc/14823>
- Ferraccioli, F., Jones, P., Vaughan, A., & Leat, P. (2006). New aerogeophysical view of the Antarctic Peninsula: More pieces, less puzzle. *Geophysical Research Letters*, 33(5), L05310. <https://doi.org/10.1029/2005gl024636>
- Ferraccioli, F., Jones, P. C., Curtis, M. L., Leat, P. T., & Riley, T. R. (2005). Tectonic and magmatic patterns in the Jutulstraumen rift (?) region, East Antarctica, as imaged by high-resolution aeromagnetic data. *Earth Planets and Space*, 57(8), 767–780. <https://doi.org/10.1186/bf03351856>
- Ferraccioli, F., von Frese, R. R. B., Ghidella, M., & Thybo, H. (2013). Recent Advances in Antarctic Geomagnetism and Lithosphere studies—Preface. *Tectonophysics*, 585, 1–206. <https://doi.org/10.1016/j.tecto.2012.11.002>
- Finn, C. A., Goodge, J. W., Damaske, D., & Fanning, C. M. (2006). Scouting craton's edge in Paleo-Pacific Gondwana. In D. K. Futterer, D. Damaske, G. Gleinschmidt, H. Miller, & F. Tessensohn (Eds.), *Antarctica: Contributions to global earth sciences* (pp. 165–173). Springer-Verlag.
- Finn, C. A., Moore, D., Damaske, D., & Mackey, T. (1999). Aeromagnetic legacy of early Paleozoic subduction along the Pacific margin of Gondwana. *Geology*, 27(12), 1087–1090. [https://doi.org/10.1130/0091-7613\(1999\)027<1087:aloeps>2.3.co;2](https://doi.org/10.1130/0091-7613(1999)027<1087:aloeps>2.3.co;2)
- Forsberg, R., Olesen, A. V., Ferraccioli, F., Jordan, T. A., Matsuoka, K., Zakrajsek, A., et al. (2018). Exploring the Recovery Lakes region and interior Dronning Maud Land, East Antarctica, with airborne gravity, magnetic and radar measurements. *Geological Society, London, Special Publications*, 461(1), 23–34. <https://doi.org/10.1144/sp461.17>
- Foss, C., Heath, P., Dutch, R., Wise, T., Pawley, M., & Reed, G. (2018). Coompana gravity and magnetic studies. In *Presented at the Coompana drilling and geochemistry workshop 2018 extended abstracts* (Vol. 19, pp. 41–50). Report Book.
- Foss, C., Reed, G., Heath, P., Dutch, R., & Wise, T. (2016). Investigation of the Coompana negative magnetic anomaly in southwestern South Australia. In *Uncover earth's past to discover our future* (p. 149).
- Frey, F. A., Coffin, M., Wallace, P., Weis, D., Zhao, X., Wise, S., Jr, et al. (2000). Origin and evolution of a submarine large igneous province: The Kerguelen Plateau and broken ridge, southern Indian Ocean. *Earth and Planetary Science Letters*, 176(1), 73–89. [https://doi.org/10.1016/S0012-821X\(99\)00315-5](https://doi.org/10.1016/S0012-821X(99)00315-5)
- Gaina, C., Müller, R. D., Brown, B., Ishihara, T., & Ivanov, S. (2007). Breakup and early seafloor spreading between India and Antarctica. *Geophysical Journal International*, 170(1), 151–169. <https://doi.org/10.1111/j.1365-246x.2007.03450.x>
- Gapais, D., Pelletier, A., Ménot, R.-P., & Peucat, J.-J. (2008). Paleoproterozoic tectonics in the Terre Adélie Craton (East Antarctica). *Precambrian Research*, 162(3–4), 531–539. <https://doi.org/10.1016/j.precamres.2007.10.011>
- Gardner, R. L., Daczko, N. R., Halpin, J. A., & Whittaker, J. M. (2015). Discovery of a microcontinent (Gulden Draak Knoll) offshore Western Australia: Implications for East Gondwana reconstructions. *Gondwana Research*, 28(3), 1019–1031. <https://doi.org/10.1016/j.gr.2014.08.013>
- Garrett, S., Herrod, L., & Mantripp, D. (1987). Crustal structure of the area around Haag Nunataks, West Antarctica: New aeromagnetic and bedrock elevation data. *Gondwana Six: Structure, Tectonics, and Geophysics*, 40, 109–115. <https://doi.org/10.1029/GM040p0109>
- Ghidella, M., Zambrano, O., Ferraccioli, F., Lirio, J., Zakrajsek, A., Ferris, J., & Jordan, T. (2013). Analysis of James Ross Island volcanic complex and sedimentary basin based on high-resolution aeromagnetic data. *Tectonophysics*, 585, 90–101. <https://doi.org/10.1016/j.tecto.2012.06.039>
- Gohl, K., Denk, A., Eagles, G., & Wobbe, F. (2013). Deciphering tectonic phases of the Amundsen Sea Embayment shelf, West Antarctica, from a magnetic anomaly grid. *Tectonophysics*, 585, 113–123. <https://doi.org/10.1016/j.tecto.2012.06.036>
- Golynsky, A. V. (2007). Magnetic anomalies in East Antarctica and surrounding regions: A window on major tectonic provinces and their boundaries. In A. K. Cooper, C. R. Raymond, & ISAES Editorial Team. (Eds.), *Antarctica: A keystone in a changing world* (Vol. 1047). The National Academies Press.
- Golynsky, A. V., & Aleshkova, N. D. (2000). New aspects of crustal structure in the Weddell Sea region from aeromagnetic studies. *Polarforschung*, 67(3), 133–141.
- Golynsky, A. V., Alyavdin, S., Masolov, V., Tschernin, A., & Volnukhin, V. (2002). The composite magnetic anomaly map of the East Antarctic. *Tectonophysics*, 347(1–3), 109–120. [https://doi.org/10.1016/S0040-1951\(01\)00240-2](https://doi.org/10.1016/S0040-1951(01)00240-2)
- Golynsky, A. V., Blankenship, D., Chiappini, M., Damaske, D., Ferraccioli, F., Finn, C., et al. (2007). New magnetic anomaly map of East Antarctica and surrounding regions. In A. K. Cooper, C. R. Raymond, & ISAES Editorial Team. (Eds.), *Antarctica: A keystone in a changing world* (p. 050). The National Academies Press. <https://doi.org/10.3133/ofr20071047srp050>
- Golynsky, A. V., Chiappini, M., Damaske, D., Ferraccioli, F., Ferris, J., Finn, C., et al. (2001). ADMAP—Magnetic Anomaly map of the Antarctic, 1: 10 000 000 scale map. *BAS (Misc.)*, 10, 1109–1112.
- Golynsky, A. V., Ferraccioli, F., Hong, J., Golynsky, D., von Frese, R., Young, D., et al. (2018). New magnetic anomaly map of the Antarctic. *Geophysical Research Letters*, 45(13), 6437–6449. <https://doi.org/10.1029/2018gl078153>
- Golynsky, A. V., Golynsky, D., Ferraccioli, F., Jordan, T., Blankenship, D., Holt, J., et al. (2017). *ADMAP-2: Magnetic anomaly map of the Antarctic*. (Map 1, scale 1: 10 000 000). Korea Polar Research Institute.
- Golynsky, A. V., Golynsky, D. A., & Kiselev, A. V. (2021, in preparation). *The location of the Kuunga suture based on new Russian aeromagnetic data*.

- Golynsky, A. V., Golynsky, D. A., Masolov, V. N., & Volnukhin, V. S. (2006). Magnetic anomalies of the Grove Mountains region and their geological significance. In D. K. Futterer, D. Damaske, G. Gleinschmidt, H. Miller, & F. Tessensohn (Eds.), *Antarctica: Contributions to global earth sciences* (pp. 95–105). Springer-Verlag.
- Golynsky, A. V., Golynsky, D. A., & von Frese, R. R. B. (2021). Compiling ship and airborne measurements for the Antarctic's second-generation magnetic anomaly map. In-review. *Russian Journal of Earth Sciences*.
- Golynsky, A. V., Ivanov, S., Kazankov, A. J., Jokat, W., Masolov, V., von Frese, R. R. B., & ADMAP Working Group. (2013). New continental margin magnetic anomalies of East Antarctica. *Tectonophysics*, 585, 172–184. <https://doi.org/10.1016/j.tecto.2012.06.043>
- Golynsky, A. V., & Jacobs, J. (2001). Grenville-age versus pan-african magnetic anomaly imprints in Western Dronning Maud Land, East Antarctica. *The Journal of Geology*, 109(1), 136–142. <https://doi.org/10.1086/317964>
- Golynsky, A. V., Masolov, V. N., Nogi, Y., Shibuya, K., Tarlowsky, C., & Wellman, P. (1996). Magnetic anomalies of Precambrian terranes of the East Antarctic shield coastal region (20°E–50°E). *Presented at the proceedings of the NIPR symposium on Antarctic Geoscience* (Vol. 9, pp. 24–39).
- Golynsky, A. V., Masolov, V. N., Volnukhin, V. S., & Golynsky, D. A. (2006). Crustal provinces of the Prince Charles Mountains region and surrounding areas in the light of aeromagnetic data. In *Antarctica* (pp. 83–94). Springer.
- Golynsky, A. V., Morris, P., Kovacs, L., & Ferris, J. (2002). A new magnetic map of the Weddell Sea and the Antarctic Peninsula. *Tectonophysics*, 347(1–3), 3–11. [https://doi.org/10.1016/s0040-1951\(01\)00234-7](https://doi.org/10.1016/s0040-1951(01)00234-7)
- Golynsky, D. A., & Golynsky, A. V. (2007). Gaussberg rift—illusion or reality. In *10th international symposium on Antarctic earth sciences, USGS open-file rep. 2007-1047, extended abstract* (Vol. 168, p. 5). The National Academies Press. Retrieved from <http://pubs.usgs.gov/of/2007/1047/ea/of2007-1047ea168.pdf>
- Golynsky, D. A., & Golynsky, A. V. (2012). East Antarctic rift systems—key to understanding of Gondwana break-up. In *Presented at the EGU general assembly conference abstracts* (p. 10001).
- Goode, J. W., & Finn, C. A. (2010). Glimpses of East Antarctica: Aeromagnetic and satellite magnetic view from the central Transantarctic Mountains of East Antarctica. *Journal of Geophysical Research*, 115(B9), B09103. <https://doi.org/10.1029/2009jb006890>
- Goode, J. W., Williams, I. S., & Myrow, P. (2004). Provenance of Neoproterozoic and lower Paleozoic siliciclastic rocks of the central Ross orogen, Antarctica: Detrital record of rift-, passive-, and active-margin sedimentation. *Geological Society of America Bulletin*, 116(9–10), 1253–1279. <https://doi.org/10.1130/b25347.1>
- Gose, W. A., Helper, M. A., Connelly, J. N., Hutson, F. E., & Dalziel, I. W. (1997). Paleomagnetic data and U-Pb isotopic age determinations from Coats Land, Antarctica: Implications for late Proterozoic plate reconstructions. *Journal of Geophysical Research*, 102(B4), 7887–7902. <https://doi.org/10.1029/96jb03595>
- Granot, R., Cande, S., Stock, J., & Damaske, D. (2013). Revised Eocene-Oligocene kinematics for the West Antarctic Rift system. *Geophysical Research Letters*, 40(2), 279–284. <https://doi.org/10.1029/2012gl054181>
- Grantham, G., & Hunter, D. (1991). The timing and nature of faulting and jointing adjacent to the Pencksökket, western Dronning Maud Land, Antarctica. *Geological Evolution of Antarctica*, 1, 47.
- Grikurov, G. E., & Leychenkov, G. L. (2012). *Tectonic map of Antarctica. 1: 10 M scale, CGMW, Paris, 1 sheet*. Retrieved from <https://ccgm.org/en/catalogue/125-carte-tectonique-de-l-antarctique-9782917310151.html>
- Groenewald, P., Grantham, G., & Watkeys, M. (1991). Geological evidence for a Proterozoic to Mesozoic link between southeastern Africa and Dronning Maud Land, Antarctica. *Journal of the Geological Society*, 148(6), 1115–1123. <https://doi.org/10.1144/gsjgs.148.6.1115>
- Haagmans, R., Menard, Y., Floberghagen, R., Plank, G., & Drinkwater, M. (2010). Swarm: ESA's magnetic field mission. In *Presented at the AGU fall meeting abstracts* (Vol. 2010, pp. GP21A–0984).
- Hinze, W. J., von Frese, R. R., & Saad, A. H. (2013). *Gravity and magnetic exploration: Principles, practices, and applications*. Cambridge University Press.
- Hittleman, A. M., Buhmann, R. W., & Racey, S. D. (1996). *Project Magnet data (1953–1994) CD-ROM User's manual*.
- Jacobs, J., Bauer, W., Spaeth, G., Thomas, R., & Weber, K. (1996). Lithology and structure of the Grenville-aged (≈1.1 Ga) basement of Heimfrontjella (East Antarctica). *Geologische Rundschau*, 85(4), 800–821. <https://doi.org/10.1007/bf02440112>
- Jacobs, J., Elburg, M., Läufer, A., Kleinhanns, I. C., Henjes-Kunst, F., Estrada, S., et al. (2015). Two distinct late Mesoproterozoic/early Neoproterozoic basement provinces in central/eastern Dronning Maud Land, East Antarctica: The missing link, 15–21°E. *Precambrian Research*, 265, 249–272. <https://doi.org/10.1016/j.precamres.2015.05.003>
- Jacobs, J., Fanning, C. M., & Bauer, W. (2003). Timing of Grenville-age vs. Pan-African medium-to high grade metamorphism in western Dronning Maud Land (East Antarctica) and significance for correlations in Rodinia and Gondwana. *Precambrian Research*, 125(1–2), 1–20. [https://doi.org/10.1016/s0301-9268\(03\)00048-2](https://doi.org/10.1016/s0301-9268(03)00048-2)
- Jacobs, J., Fanning, C. M., Henjes-Kunst, F., Olesch, M., & Paech, H.-J. (1998). Continuation of the Mozambique belt into East Antarctica: Grenville-age metamorphism and polyphase Pan-African high-grade events in central Dronning Maud Land. *The Journal of Geology*, 106(4), 385–406. <https://doi.org/10.1086/516031>
- Jacobs, J., & Thomas, R. J. (2004). Himalayan-type indenter-escape tectonics model for the southern part of the late Neoproterozoic–early Paleozoic East African–Antarctic orogen. *Geology*, 32(8), 721–724. <https://doi.org/10.1130/g20516.1>
- Jankowski, E., Drewry, D., & Behrendt, J. (1983). Magnetic studies of upper crustal structure in West Antarctica and the boundary with East Antarctica. *Antarctic Earth Science*, 197–203.
- Johnson, A. C. (1999). Interpretation of new aeromagnetic anomaly data from the central Antarctic Peninsula. *Journal of Geophysical Research*, 104(B3), 5031–5046. <https://doi.org/10.1029/1998jb900073>
- Johnson, A. C., von Frese, R., & ADMAP Working Group. (1997). Magnetic map will define Antarctica's structure. *Eos, Transactions American Geophysical Union*, 78(18), 185. <https://doi.org/10.1029/97eo00123>
- Jokat, W., Boebel, T., König, M., & Meyer, U. (2003). Timing and geometry of early Gondwana breakup. *Journal of Geophysical Research*, 108(B9), 2428. <https://doi.org/10.1029/2002jb001802>
- Jokat, W., Nogi, Y., & Leinweber, V. (2010). New aeromagnetic data from the western Enderby Basin and consequences for Antarctic-India break-up. *Geophysical Research Letters*, 37(21), L21311. <https://doi.org/10.1029/2010gl045117>
- Jordan, T. A., Ferraccioli, F., & Leat, P. (2017). New geophysical compilations link crustal block motion to Jurassic extension and strike-slip faulting in the Weddell Sea Rift System of West Antarctica. *Gondwana Research*, 42, 29–48. <https://doi.org/10.1016/j.gr.2016.09.009>
- Jordan, T. A., Ferraccioli, F., Ross, N., Corr, H. F., Leat, P. T., Bingham, R. G., et al. (2013). Inland extent of the Weddell Sea Rift imaged by new aerogeophysical data. *Tectonophysics*, 585, 137–160. <https://doi.org/10.1016/j.tecto.2012.09.010>
- Jordan, T. A., Ferraccioli, F., Vaughan, D., Holt, J., Corr, H., Blankenship, D., & Diehl, T. (2010). Aerogravity evidence for major crustal thinning under the Pine Island Glacier region (West Antarctica). *Bulletin*, 122(5–6), 714–726. <https://doi.org/10.1130/b26417.1>

- Jordan, T. A., Neale, R., Leat, P., Vaughan, A., Flowerdew, M., Riley, T., et al. (2014). Structure and evolution of Cenozoic arc magmatism on the Antarctic Peninsula: A high resolution aeromagnetic perspective. *Geophysical Journal International*, 198(3), 1758–1774. <https://doi.org/10.1093/gji/ggu233>
- Kamenev, E., Andronikov, A., Mikhalsky, E., Krasnikov, N., & Stüwe, K. (1993). Soviet geological maps of the Prince Charles mountains, East Antarctic shield. *Australian Journal of Earth Sciences*, 40(5), 501–517. <https://doi.org/10.1080/08120099308728100>
- Kim, H. R., & von Frese, R. R. (2017). Utility of Slepian basis functions for modeling near-surface and satellite magnetic anomalies of the Australian lithosphere. *Earth Planets and Space*, 69(1), 53. <https://doi.org/10.1186/s40623-017-0636-0>
- Kim, H. R., von Frese, R. R., Golynsky, A. V., Taylor, P. T., & Kim, J. W. (2004). Application of satellite magnetic observations for estimating near-surface magnetic anomalies. *Earth Planets and Space*, 56(10), 955–966. <https://doi.org/10.1186/bf03351793>
- Kim, H. R., von Frese, R. R. B., Taylor, P. T., Golynsky, A. V., Gaya-Piqué, L. R., & Ferraccioli, F. (2007). Improved magnetic anomalies of the Antarctic lithosphere from satellite and near-surface data. *Geophysical Journal International*, 171(1), 119–126. <https://doi.org/10.1111/j.1365-246x.2007.03516.x>
- Kim, J. W., Kim, H. R., von Frese, R. R. B., Taylor, P., & Rangelova, E. (2013). Geopotential field anomaly continuation with multi-altitude observations. *Tectonophysics*, 585, 34–47. <https://doi.org/10.1016/j.tecto.2012.07.016>
- Kleinschmidt, G., & Buggisch, W. (1994). Plate tectonic implications of the structure of the Shackleton Range, Antarctica. *Polarforschung*, 63(1), 57–62.
- Kleinschmidt, G., Buggisch, W., Läufer, A., Helfferich, S., Tessensohn, F., Gamble, J., et al. (2002). The “Ross orogenic” structures in the Shackleton Range and their meaning for Antarctica. In *Antarctica at the close of a millennium* (Vol. 35, pp. 75–83). Royal Society of New Zealand.
- König, M., & Jokat, W. (2006). The mesozoic breakup of the Weddell sea. *Journal of Geophysical Research*, 111(B12), B12102. <https://doi.org/10.1029/2005JB004035>
- Kovacs, L. C., Morris, P., Brozena, J., & Tikku, A. (2002). Seafloor spreading in the Weddell Sea from magnetic and gravity data. *Tectonophysics*, 347(1–3), 43–64. [https://doi.org/10.1016/S0040-1951\(01\)00237-2](https://doi.org/10.1016/S0040-1951(01)00237-2)
- LaBrecque, J., Cande, S., Bell, R., Raymond, C., Brozena, J., Keller, M., et al. (1986). *Aerogeophysical survey yields new data in the Weddell Sea*.
- Laiba, A., & Kudriavtsev, I. (2006). Geological observations of the eastern fringe of the Amery ice shelf during the 49-th Russian Antarctic Expedition. *Russian Earth Science Research in Antarctica*, 1, 33–53.
- Leinweber, V. T., & Jokat, W. (2012). The Jurassic history of the Africa–Antarctica corridor—New constraints from magnetic data on the conjugate continental margins. *Tectonophysics*, 530, 87–101. <https://doi.org/10.1016/j.tecto.2011.11.008>
- Leitchenkov, G., Guseva, J., Gandyukhin, V., Grikurov, G., Kristoffersen, Y., Sand, M., et al. (2008). Crustal structure and tectonic provinces of the Riiser-Larsen Sea area (East Antarctica): Results of geophysical studies. *Marine Geophysical Researches*, 29(2), 135–158. <https://doi.org/10.1007/s11001-008-9051-z>
- LeMasurier, W. (1990). Late Cenozoic volcanism on the Antarctic Plate: An overview. *Volcanoes of the Antarctic Plate and Southern Oceans*, 48, 1–17. <https://doi.org/10.1029/ar048p0001>
- Liu, X., Jahn, B., Zhao, Y., Liu, J., & Ren, L. (2014). Geochemistry and geochronology of Mesoproterozoic basement rocks from the Eastern Amery ice shelf and southwestern Prydz Bay, East Antarctica: Implications for a long-lived magmatic accretion in a continental arc. *American Journal of Science*, 314(2), 508–547. <https://doi.org/10.2475/02.2014.03>
- Liu, X., Zhao, Y., Liu, J., Chen, H., Cui, Y., & Song, B. (2016). Early Mesoproterozoic arc magmatism followed by early Neoproterozoic granulite facies metamorphism with a near-isobaric cooling path at Mount Brown, Princess Elizabeth Land, East Antarctica. *Precambrian Research*, 284, 30–48. <https://doi.org/10.1016/j.precamres.2016.08.003>
- Loewy, S., Dalziel, I., Pisarevsky, S., Connelly, J., Tait, J., Hanson, R., & Bullen, D. (2011). Coats Land crustal block, East Antarctica: A tectonic tracer for Laurentia? *Geology*, 39(9), 859–862. <https://doi.org/10.1130/g32029.1>
- Luyendyk, B. P., Wilson, D. S., & Siddoway, C. S. (2003). Eastern margin of the Ross Sea rift in western Marie Byrd Land, Antarctica: Crustal structure and tectonic development. *Geochemistry, Geophysics, Geosystems*, 4(10), 1090. <https://doi.org/10.1029/2002gc000462>
- Maritati, A., Aitken, A. R. A., Young, D., Roberts, J., Blankenship, D., & Siegert, M. (2016). The tectonic development and erosion of the Knox subglacial sedimentary basin, East Antarctica. *Geophysical Research Letters*, 43(20), 10–728. <https://doi.org/10.1002/2016gl071063>
- Maritati, A., Halpin, J. A., Whittaker, J. M., & Daczko, N. R. (2019). Fingerprinting Proterozoic bedrock in interior Wilkes Land, East Antarctica. *Scientific Reports*, 9(1), 1–12. <https://doi.org/10.1038/s41598-019-46612-y>
- Maslanyj, M., Smith, A., & Garrett, S. (1991). *Aeromagnetic anomaly map of West Antarctica (Weddell Sea sector) 1: 2 500 000*. [No Source Information Available].
- Maslanyj, M., & Storey, B. (1990). Regional aeromagnetic anomalies in Ellsworth Land: Crustal structure and Mesozoic microplate boundaries within West Antarctica. *Tectonics*, 9(6), 1515–1532. <https://doi.org/10.1029/tc009i006p01515>
- Maus, S., Barckhausen, U., Berkenbosch, H., Bournas, N., Brozena, J., Childers, V., et al. (2009). EMAG2: A 2–arc min resolution Earth magnetic Anomaly Grid compiled from satellite, airborne, and marine magnetic measurements. *Geochemistry, Geophysics, Geosystems*, 10(8), Q08005. <https://doi.org/10.1029/2009gc002471>
- Mawson, D. (1940). Australasian Antarctic Expedition, 1911–1914. *The Geographical Journal*, 44(3), 257–284.
- McEnroe, S. A., & Brown, L. L. (2000). A closer look at remanence-dominated aeromagnetic anomalies: Rock magnetic properties and magnetic mineralogy of the Russell Belt microcline-sillimanite gneiss, northwest Adirondack Mountains, New York. *Journal of Geophysical Research*, 105(B7), 16437–16456. <https://doi.org/10.1029/2000jb900051>
- McEnroe, S. A., Robinson, P., & Panish, P. T. (2001). Aeromagnetic anomalies, magnetic petrology, and rock magnetism of hemo-ilmenite- and magnetite-rich cumulate rocks from the Sokndal Region, South Rogaland, Norway. *American Mineralogist*, 86(11–12), 1447–1468. <https://doi.org/10.2138/am-2001-11-1213>
- McLean, M., Wilson, C., Boger, S., Betts, P. G., Rawling, T., & Damaske, D. (2009). Basement interpretations from airborne magnetic and gravity data over the Lambert Rift region of East Antarctica. *Journal of Geophysical Research*, 114(B6), B06101. <https://doi.org/10.1029/2008jb005650>
- Mezger, K., & Cosca, M. A. (1999). The thermal history of the Eastern Ghats belt (India) as revealed by U–Pb and 40Ar/39Ar dating of metamorphic and magmatic minerals: Implications for the SWEAT correlation. *Precambrian Research*, 94(3–4), 251–271. [https://doi.org/10.1016/S0301-9268\(98\)00118-1](https://doi.org/10.1016/S0301-9268(98)00118-1)
- Mieth, M., Jacobs, J., Ruppel, A., Damaske, D., Läufer, A., & Jokat, W. (2014). New detailed aeromagnetic and geological data of eastern Dronning Maud Land: Implications for refining the tectonic and structural framework of Sør Rondane, East Antarctica. *Precambrian Research*, 245, 174–185. <https://doi.org/10.1016/j.precamres.2014.02.009>
- Mieth, M., & Jokat, W. (2014). New aeromagnetic view of the geological fabric of southern Dronning Maud Land and Coats Land, East Antarctica. *Gondwana Research*, 25(1), 358–367. <https://doi.org/10.1016/j.gr.2013.04.003>

- Mikhalsky, E., Belyatsky, B., Presnyakov, S., Skublov, S., Kovach, V., Rodionov, N., et al. (2015). The geological composition of the hidden Wilhelm II Land In East Antarctica: SHRIMP zircon, Nd isotopic and geochemical studies with implications for Proterozoic supercontinent reconstructions. *Precambrian Research*, 258, 171–185. <https://doi.org/10.1016/j.precamres.2014.12.011>
- Mikhalsky, E., Sheraton, J., Kudriavtsev, I., Sergeev, S., Kovach, V., Kamenev, I., & Laiba, A. (2013). The Mesoproterozoic Rayner Province in the Lambert Glacier area: Its age, origin, isotopic structure and implications for Australia–Antarctica correlations. *Geological Society, London, Special Publications*, 383(1), 35–57. <https://doi.org/10.1144/sp383.1>
- Mikhalsky, E., Sheraton, J., Laiba, A., & Beliatsky, B. (1996). Geochemistry and origin of Mesoproterozoic metavolcanic rocks from Fisher Massif, Prince Charles mountains, East Antarctica. *Antarctic Science*, 8(1), 85–104. <https://doi.org/10.1017/s0954102096000120>
- Milligan, P., Franklin, R., Minty, B., Richardson, L., & Percival, P. (2010). Magnetic Anomaly Map of Australia: Canberra, Geoscience Australia. scale: 1: 15,000,000.
- Mukasa, S. B., & Dalziel, I. W. (2000). Marie Byrd Land, West Antarctica: Evolution of Gondwana's Pacific margin constrained by zircon U–Pb geochronology and feldspar common-Pb isotopic compositions. *Geological Society of America Bulletin*, 112(4), 611–627. [https://doi.org/10.1130/0016-7606\(2000\)112<611:mblwae>2.0.co;2](https://doi.org/10.1130/0016-7606(2000)112<611:mblwae>2.0.co;2)
- Mulder, J. A., Halpin, J. A., Daczko, N. R., Orth, K., Meffre, S., Thompson, J. M., & Morrissey, L. J. (2019). A Multiproxy provenance approach to uncovering the assembly of East Gondwana in Antarctica. *Geology*, 47(7), 645–649. <https://doi.org/10.1130/g45952.1>
- Müller, R. D., Sdrolias, M., Gaina, C., & Roest, W. R. (2008). Age, spreading rates, and spreading asymmetry of the world's ocean crust. *Geochemistry, Geophysics, Geosystems*, 9(4), Q04006. <https://doi.org/10.1029/2007GC001743>
- Nogi, Y., Jokat, W., Kitada, K., & Steinhage, D. (2013). Geological structures inferred from airborne geophysical surveys around Lützow-Holm Bay, East Antarctica. *Precambrian Research*, 234, 279–287. <https://doi.org/10.1016/j.precamres.2013.02.008>
- Olsen, N., Ravat, D., Finlay, C. C., & Kother, L. K. (2017). LCS-1: A high-resolution global model of the lithospheric magnetic field derived from CHAMP and Swarm satellite observations. *Geophysical Journal International*, 211(3), 1461–1477. <https://doi.org/10.1093/gji/ggx381>
- Paech, H., & Marcinkowski, V. (2005). Magnetic susceptibility of rock samples from Central Dronning Maud Land, East Antarctica. *Geologisches Jahrbuch - Reihe B*, 97, 85.
- Paterson, N. R., Reford, S. W., & Kwan, K. C. (1990). Continuation of magnetic data between arbitrary surfaces: Advances and applications. In *SEG technical program expanded abstracts 1990* (pp. 666–669). Society of Exploration Geophysicists. <https://doi.org/10.1190/1.1890296>
- Pavlov, V. (1958). Results of palynological analysis of samples from the sedimentaryvolcanic Beacon series (Antarctica, King George V Coast, Horn Bluff). *Nauk-Issl Institute of Geology Arktiki. Sbornik Stratigraphy. Palaeontology and Biostratigraphy*, 12(77), 9.
- Payne, J. L., Hand, M., Barovich, K. M., Reid, A., & Evans, D. A. (2009). Correlations and reconstruction models for the 2500–1500 Ma evolution of the Mawson Continent. *Geological Society, London, Special Publications*, 323(1), 319–355. <https://doi.org/10.1144/sp323.16>
- Ravich, M. G., Klimov, L., & Solov'ev, D. (1968). *The Pre-Cambrian of East Antarctica* (Vol. 67). Israel Program for Scientific Translations [available from the US Department].
- Ravich, M. G., Solov'ev, D., & Fedorov, L. (1985). *Geological structure of Mac. Robertson Land (East Antarctica)*. *Gidrometeoizdat*.
- Riedel, S., Jacobs, J., & Jokat, W. (2013). Interpretation of new regional aeromagnetic data over Dronning Maud Land (East Antarctica). *Tectonophysics*, 585, 161–171. <https://doi.org/10.1016/j.tecto.2012.10.011>
- Ruppel, A., Jacobs, J., Eagles, G., Läufer, A., & Jokat, W. (2018). New geophysical data from a key region In East Antarctica: Estimates for the spatial extent of the Tonian oceanic arc super terrane (TOAST). *Gondwana Research*, 59, 97–107. <https://doi.org/10.1016/j.gr.2018.02.019>
- Schmadecke, E., & Will, T. M. (2006). First evidence of eclogite facies metamorphism in the Shackleton range, Antarctica: Trace of a suture between East and West Gondwana? *Geology*, 34(3), 133–136. <https://doi.org/10.1130/g22170.1>
- Sergeyev, M., Mikhailov, V., Meyer, U., & Eckstaller, A. (1999). The geological nature of the Haskard-Fuchs magnetic anomaly and an identification of highly-magnetic rock units in the Shackleton Range, Antarctica. *Terra Antarctica*, 6(3–4), 327–336.
- Shiraiishi, K., Ellis, D., Hiroi, Y., Fanning, C., Motoyoshi, Y., & Nakai, Y. (1994). Cambrian orogenic belt In East Antarctica and Sri Lanka: Implications for Gondwana assembly. *The Journal of Geology*, 102(1), 47–65. <https://doi.org/10.1086/629647>
- Smith, A. M., Jordan, T. A., Ferraccioli, F., & Bingham, R. G. (2013). Influence of subglacial conditions on ice stream dynamics: Seismic and potential field data from Pine Island Glacier, West Antarctica. *Journal of Geophysical Research: Solid Earth*, 118(4), 1471–1482. <https://doi.org/10.1029/2012jb009582>
- Stagg, H. M. J., Colwell, J., Direen, N., O'Brien, P., Browning, B., Bernardel, G., et al. (2005). Geological framework of the continental margin in the region of the Australian Antarctic Territory. *Geoscience Australia Record*, 2004, 1–373.
- Studinger, M., Bell, R. E., Buck, W. R., Karner, G. D., & Blankenship, D. D. (2004). Sub-ice geology inland of the Transantarctic Mountains in light of new aerogeophysical data. *Earth and Planetary Science Letters*, 220(3), 391–408. [https://doi.org/10.1016/s0012-821x\(04\)00066-4](https://doi.org/10.1016/s0012-821x(04)00066-4)
- Studinger, M., Bell, R. E., Karner, G. D., Tikku, A. A., Holt, J. W., Morse, D. L., et al. (2003). Ice cover, landscape setting, and geological framework of Lake Vostok, East Antarctica. *Earth and Planetary Science Letters*, 205(3–4), 195–210. [https://doi.org/10.1016/s0012-821x\(02\)01041-5](https://doi.org/10.1016/s0012-821x(02)01041-5)
- Talarico, F., Armadillo, E., & Bozzo, E. (2001). Antarctic rock magnetic properties: New susceptibility measurements in Oates Land and George V Land. *Terra Antarctica Reports*, 5, 45–50.
- Talarico, F., Kleinschmidt, G., & Henjes-Kunst, F. (1999). An ophiolitic complex in the northern Shackleton Range, Antarctica. *Terra Antarctica*, 6(3–4), 293–315.
- Tessensohn, F. (1997). Shackleton range, Ross orogen and SWEAT hypothesis. *The Antarctic Region: Geological Evolution and Processes*, 5–12.
- Tonarini, S., Rocchi, S., Armienti, P., & Innocenti, F. (1997). Constraints on timing of Ross Sea rifting inferred from Cenozoic intrusions from northern Victoria Land, Antarctica, in *The Antarctic Region: Geological Evolution and Processes*. In C. A. Ricci (Ed.), *Proceedings of the 7th International Symposium on Antarctic Earth Sciences* (pp. 511–521).
- Vaughan, A. P., Eagles, G., & Flowerdew, M. J. (2012). Evidence for a two-phase Palmer Land event from crosscutting structural relationships and emplacement timing of the Lassiter Coast intrusive suite, Antarctic Peninsula: Implications for mid-Cretaceous Southern Ocean plate configuration. *Tectonics*, 31(1), TC1010. <https://doi.org/10.1029/2011Tc003006>
- von Frese, R., Hinze, W., Braile, L., & Luca, A. (1981). Spherical-earth gravity and magnetic anomaly modeling by Gauss-Legendre quadrature integration. *Journal of Geophysics*, 49, 234–242.
- von Frese, R., Kim, H., Leftwich, T., Kim, J., & Golynsky, A. (2013). Satellite magnetic anomalies of the Antarctic Wilkes Land impact basin inferred from regional gravity and terrain data. *Tectonophysics*, 585, 185–195. <https://doi.org/10.1016/j.tecto.2012.09.009>
- von Frese, R. R., Potts, L. V., Wells, S. B., Leftwich, T. E., Kim, H. R., Kim, J. W., et al. (2009). GRACE gravity evidence for an impact basin in Wilkes Land, Antarctica. *Geochemistry, Geophysics, Geosystems*, 10(2), Q02014. <https://doi.org/10.1029/2008gc002149>
- von Frese, R. R. B. (1998). Correction to: R. R. B. von Frese, W. J. Hinze, L. W. Braile, "Spherical Earth gravity and magnetic anomaly analysis by equivalent point source inversion". *Earth and Planetary Science Letters*, 163(1), 409–411. [https://doi.org/10.1016/S0012-821X\(98\)00174-5](https://doi.org/10.1016/S0012-821X(98)00174-5)

- von Frese, R. R. B., Golynsky, A. V., Kim, H. R., Gaya-Piqué, L., Thébault, E., Chiappini, M., et al. (2008). The next generation Antarctic digital magnetic anomaly map. In A. K. Cooper, & C. R. Raymond (Eds.), *Proceedings of the 10th ISAES, USGS open-file report 2007-1047*. <https://doi.org/10.3133/of2007.srp163>
- von Frese, R. R. B., Hinze, W. J., Olivier, R., & Bentley, C. R. (1986). Regional magnetic anomaly constraints on continental breakup. *Geology*, *14*(1), 68–71. [https://doi.org/10.1130/0091-7613\(1986\)14<68:rmacoc>2.0.co;2](https://doi.org/10.1130/0091-7613(1986)14<68:rmacoc>2.0.co;2)
- von Frese, R. R. B., Taylor, P. T., & Chiappini, M. (2002). Preface. *Tectonophysics*, *347*(1), 1–2. [https://doi.org/10.1016/S0040-1951\(01\)00233-5](https://doi.org/10.1016/S0040-1951(01)00233-5)
- Will, T., Frimmel, H., Zeh, A., Le Roux, P., & Schmädicke, E. (2010). Geochemical and isotopic constraints on the tectonic and crustal evolution of the Shackleton Range, East Antarctica, and correlation with other Gondwana crustal segments. *Precambrian Research*, *180*(1–2), 85–112. <https://doi.org/10.1016/j.precamres.2010.03.005>
- Will, T. M., Zeh, A., Gerdes, A., Frimmel, H. E., Millar, I. L., & Schmädicke, E. (2009). Palaeoproterozoic to Palaeozoic magmatic and metamorphic events in the Shackleton Range, East Antarctica: Constraints from zircon and monazite dating, and implications for the amalgamation of Gondwana. *Precambrian Research*, *172*, 25–45. <https://doi.org/10.1016/j.precamres.2009.03.008>
- Wise, T., Pawley, M. J., & Dutch, R. A. (2016). Preliminary interpretations from the 2015 Coompana aeromagnetic survey. *ASEG Extended Abstracts*, *2016*(1), 1–6. <https://doi.org/10.1071/aseg2016ab191>
- Wobbe, F., Gohl, K., Chambord, A., & Sutherland, R. (2012). Structure and breakup history of the rifted margin of West Antarctica in relation to Cretaceous separation from Zealandia and Bellingshausen plate motion. *Geochemistry, Geophysics, Geosystems*, *13*(4), Q04W12. <https://doi.org/10.1029/2011gc003742>
- Young, D., Quartini, E., & Blankenship, D. (2017). Magnetic anomaly data over central Marie Byrd Land, West Antarctica (GIMBLE.GMGEO2) [Data set]. U.S. Antarctic Program (USAP) Data Center. <https://doi.org/10.15784/601002>
- Yu, H., Kim, H. R., von Frese, R. R. B., Golynsky, A. V., Park, K. J., & Hong, J. K. (2019). Augmenting coverage gaps in the ADMAP-2 grid with Swarm satellite magnetic observations. In *Presented at the ISEAS 2019* (p. A363). Korea Polar Institute.
- Yuasa, M., Niida, K., Ishihara, T., Kisimoto, K., & Murakami, F. (1997). Peridotite dredged from a seamount off Wilkes Land, the Antarctic: Emplacement of fertile mantle fragment at early rifting stage between Australia and Antarctica during the final breakup of Gondwanaland. *The Antarctic Region: Geological Evolution and Processes*, 725–730.
- Zengerer, M. (2017). *Coompana anomaly revisited*. Retrieved from <http://www.gondwanageo.com/>
- Zhang, C., von Frese, R. R., Shum, C., Leftwich, T. E., Kim, H. R., & Golynsky, A. V. (2020). Satellite Gravity Constraints on the Antarctic Moho and its Potential isostatic Adjustments. *Geochemistry, Geophysics, Geosystems*, *21*(12), e2020GC009048. <https://doi.org/10.1029/2020gc009048>